Roberto Baccoli[a], Federico Sollai[b], Andrea Medda[b], Antonio Piccolo[c], Paolo Fadda[b]

[a] Institute of Technical Physics, Engineering Faculty, University of Cagliari, Via Marengo 2, 09123, Cagliari, Italy
[b] Transport Institute, Engineering Faculty, University of Cagliari, Via Marengo 2, 09123, Cagliari, Italy
[c] Department of Engineering, University of Messina, Contrada di Dio, 98166, S. Agata (Messina), Italy

An Adaptive nonlinear autoregressive ANN model for high time resolution traffic noise predictions. Experimental results for a port city waterfront.

Building and Environment

Volume 207, Part B, January 2022, 108551

The publisher's version is available at:
https://doi.org/10.1016/j.buildenv.2021.108551

When citing, please refer to the published version.
Baccoli R., Sollai F., Medda A., Piccolo A., Fadda P.
AUTHOR FULL NAMES: Baccoli, Roberto; Sollai, Federico; Medda, Andrea; Piccolo, Antonio; Fadda, Paolo, An adaptive nonlinear autoregressive ANN model for high time resolution traffic noise predictions. Experimental results for a port city waterfront, (2022) Building and Environment, 207, art. no. 108551,DOI: 10.1016/j.buildenv.2021.108551

An Adaptive nonlinear autoregressive ANN model for high time resolution traffic noise predictions. Experimental results for a port city waterfront.

Roberto Baccoli[1,*], Federico Sollai[2], Andrea Medda[2], Antonio Piccolo[3], Paolo Fadda[2]

[*] corresponding author

[1]Institute of Technical Physics, Engineering Faculty, University of Cagliari, Via Marengo 2, 09123 Cagliari, Italy
[2]Transport institute, Engineering Faculty, University of Cagliari, Via Marengo 2, 09123 Cagliari, Italy
[3]Department of Engineering, University of Messina, Contrada di Dio, 98166 S. Agata (Messina) Italy

Abstract.

In this research study an adaptive recurrent artificial nonlinear neural network identification model has been developed and experimentally tested for dynamically predicting the traffic noise level $L_{eq,1'}$ with a time refinement of 1 minute. The model has been successfully applied in three selected positions, representative of the waterfront in a Mediterranean port city. Several maritime cities are exposed to a wide range of road traffic fluctuations that negatively impact liveability in the area concerned. Large volumes of road traffic periodically access the port, dynamically affecting the acoustic scenario in neighbouring areas, especially in seaside towns during the tourist season. A signalized intersection, a roundabout, and a wide entrance to a vehicular underpass have been analyzed in the course of two characteristic periods, during which traffic ranged widely from normal to peak yearly intensity. Detailed traffic data for 15 road lanes and noise sequence regressors have been considered as input data sources. This exploratory investigation reveals a good predictive performance of the model developed, the prediction error of $L_{eq,1'}$ falling prevalently within the range ±0.5dB. The experimental profile of $L_{eq,1'}$ is well reflected by the simulated sequence, and the auto and cross correlation functions confirm how well the identified neural model is able to explain the functional dependence underlying the experimental observations.

Keywords:

Traffic noise prediction model; dynamic model; nonlinear autoregressive neural network;

Nomencalture

[I] represents the neural network input matrix. It includes data about the traffic flow;

$\boldsymbol{L_{eq,1'}}$ represents the acoustic pressure level measured by the sound level meter, obtained by averaging over an integration time of 1 minute $[\mathbf{dB}]$;

$[\boldsymbol{T}]$ represents the target matrix. It includes the information of the physical quantities describing the noise level;

$\boldsymbol{\tau_i}$ represents the time at i^{th} instant $[\mathbf{min}]$;

$[t\not{f}d]$ indicates the traffic flow data. It represents the exogenous input matrix that incorporates the time sequences $\dot{V}(\tau)$, $\mathcal{v}(\tau)$ describing the temporal evolution of the flow rates and the speed for each vehicle class and lane that composes the road section, under consideration. ~~From~~

$\mathcal{v}$ average value of the different speeds of a class of vehicles measured at a given point by the traffic sensor during a time of 1 minute

$\dot{V}$ traffic flow rate in terms of vehicles per unit time crossing a considered section of a roadway lane, $\left[\frac{\text{number of vehicles}}{\text{min}}\right]$;

$|_{\boldsymbol{\tau_i}}$ denotes a physical quantity evaluated at time $\boldsymbol{\tau_i}$;

1. Introduction

Nowadays, the control and abatement of the urban noise transversally pervade the different aspects of spatial planning whereas the implications on the natural and built environment, as well as on human wellbeing have become paramount in the modern age.

Several studies of the European Environment Agency (EEA) [1] show that the dominant source of noise pollution results from road traffic. An overview of the estimated number of people that are exposed to the noise level indicators L_{den} and L_{night} equal to or exceeding the threshold values of 55 dB and 50 dB is depicted in fig. 1 for different transportation sources. Traffic noise poses severe health challenges, diminishes the quality of life and negatively impacts the livability character of the urban and indoor spaces [2] and [3]**.**

Devising specific tools for reducing noise exposure and setting proper mitigation actions can play a key role in improving the welfare of mankind. This explains why several researchers involved in applied acoustic concepts, urban planners and software developers have spawned (since the pioneering studies started in the early 1950s [4]) a plethora of studies to expedite the development of tools for traffic noise prediction.

Two classes of modelling techniques are generally adopted to determine the noise level from vehicular traffic: static and dynamic.

Static models, in the main, are oriented towards providing an acoustic representation in the spatial domain rather than over time [5-6]. For this reason, the applicability of statistical models is restricted to acoustical context where the time-varying effects are not essential. However, this approach becomes quite inadequate for reproducing the dynamic response of the acoustic field when the traffic scenario evolves continuously over short periods of time. Most conventional models accept stationary representation of the noise sources as input data, generating a corresponding crystallized timeless picture of the noise field as output, [7].

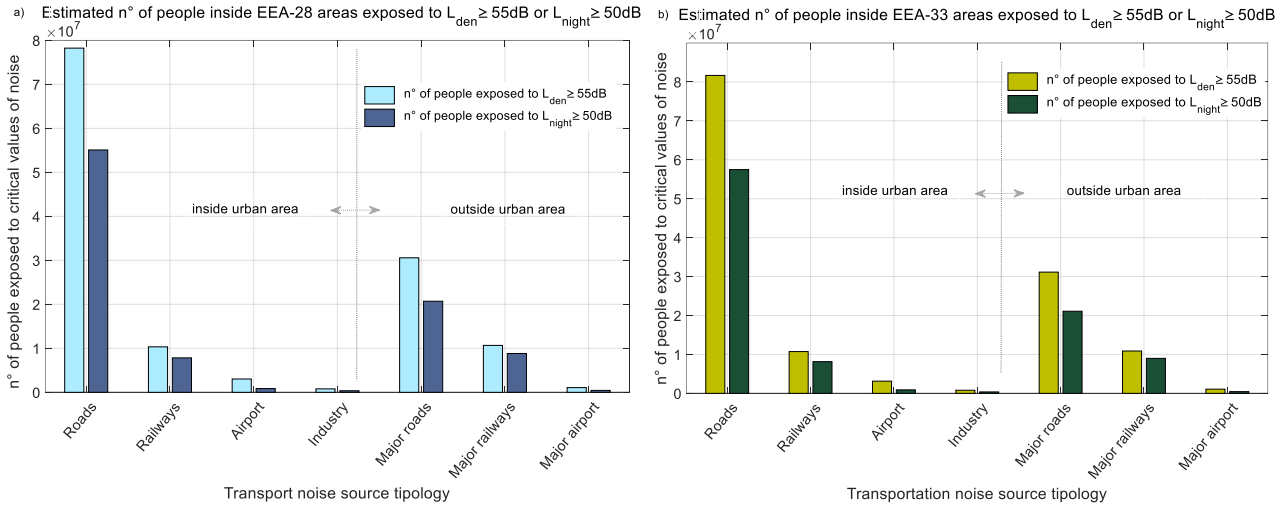

Fig. 1 Number of people exposed to values of L_{den} and L_{night} equal to or exceeding the threshold values of 55dB and 50dB, respectively. Box a) concerns people belonging to the European Union member states, while box b) refers to people belonging to the member countries of the Economic European Area. All states are counted before the Brexit decision was implemented. All data are extracted from reported data on noise exposure covered by Directive 2002/49/EC provided by European Environment Agency (EEA) and published 21 Nov 2019.

Specifically, under free-flowing traffic conditions the noise field represents the favorable scenario for noise level prediction when using static models. Conversely, non-free-flowing traffic conditions, such as at signalized intersections or roundabouts, could be critical due to the complexity inherent in the relative random influence, (as noted by S. Abo-Qudais in [8]).

A critical review and details of these standard methodologies can be found in excellent studies conducted by Naveen Garg and Sagar Maji in [9], by J. Quertieri in [10], by C. Guarnaccia et al in [11] and by C. Steel in [12]. The limitations of the static models are discussed in [7] by Quartieri et al who carried out an experimental validation of different static models, revealing a significant discrepancy between predicted and measured values.

The transition from static to dynamic prediction task has been spurred by the need to devise appropriate traffic management actions and to evaluate their impact on reducing urban noise levels [13]. Excellent studies have been proposed for new dynamic simulation models [14-15] and descriptors [16] that consider the time varying behavior of the vehicles, aimed at predicting and capturing the specific dynamics of the traffic noise [17]. Several investigations that compare dynamic versus static traffic noise representation have been proposed in [18-23], while a recent brief overview on both modeling approaches is shortly presented by G. R. Gozalo in [24].

1.1 Traffic noise prediction model based on AI.

Since the earliest study published in 1952, the advancements in the modeling approach were primarily inspired by the effort to incorporate more detail and explanatory variables into the physical description of the noise event, so as to derive an increasingly accurate, but still tractable, simulation tool. The physical approach

requires modeling the functional dependence underlying the acoustic wave phenomena. An interesting and detailed account of the existing physical approaches is presented by M. Hornikx in [25-26] and by H. Wang in [27].

Many improvements have been achieved over the decades, nevertheless accurate dynamic predictions of road traffic noise, based on a physical description approach, still remains a challenge.

During the last three decades the modeling approach has been further developed by exploring the applicability of alternative options, offered by artificial intelligence concepts, for solving road noise issues. Many methods that rely on machine learning modeling techniques can be applied for predicting the influence of vehicular traffic on urban noise. For instance, regression decision trees, support vector regression, ensembles, fuzzy logic, and artificial neural networks (ANN) methods are examined in recent studies by many authors as L. Bravo-Moncayo in [28], N. Genaro in [29], V. Nourani in [30], M. .Ali Khalil in [31], A. Sharma in [32] J. Tomić in [33], and N. Garg in [34]. The most common and successful heuristic methods are based on the ANN algorithms. Indeed, the universal applicability of ANN in modeling, classifying, controlling, and predicting complex systems with an acceptable level of accuracy, of insensitivity to noisy data and tolerance to of input data incompleteness, is one of the reasons for the recent vivid interest in developing ANN models for complex traffic noise prediction problems. Furthermore, the black-box paradigm of the neural network allows one to bypass the preliminary stage consisting in the implementation of specific physical laws of the acoustic wave propagation mechanism and related boundary conditions. This aspect is quite attractive because the preliminary stages for implementing the topographic and acoustic properties of the urban and the natural environment (with the proper refinement), in addition to noise source representation may have a significant impact on the time required for fine-tuning a physical model

At present, numerous excellent works are reported in the literature that propose theoretical and experimental validation studies employing ANN modeling techniques for traffic noise issues.

G. Cammarata in [35] and in [36] proposed a neural architecture for traffic - noise prediction in three Sicilian cities. A two-stage architecture was examined in [36]. A first preliminary stage consisting of a Learning Vector Quantization network was used for filtering measurements affected by error followed by a stage consisting of a back propagation (BP) network for predicting the pressure level. The size of the training set was equal to 70% of the entire data. The results show the proposed approach to outperform the classical relationships reported in the pertinent literature. In [37] V. Nedic et al proposed an interesting application of an ANN to traffic noise prediction. The authors adopted a feed-forward (FF) BP scheme. The ANN was trained and tested under steady-state traffic conditions on a Serbian motorway. The training and test sets comprised 70% and 30% respectively of the whole dataset. The results revealed that the ANN algorithm outperformed any other statistical method in predicting the traffic noise level. A. J. Torija et al In [38] proposed an interesting study on the use of a BP algorithm for predicting the short - term level of $L_{eq,5'}$ and the evolution, in the frequency domain, of sound pressure level for a physical characterization of the urban soundscape. Traffic features, street geometry, type of day and period, stabilization time of the sound level, and characterization of the location were considered as input data. The training, validation and test sets were equal to 80%, 5% and 15%

145 respectively of the whole dataset. A prediction error for L_{eq} lower than 1.88% and than 3.07% for the spectral
146 composition was obtained. In [39] sixteen different FF-BP ANN models were calibrated and tested by K.
147 Hamad for modeling traffic noise in a hot climate. The training and test sets size were respectively 85% and
148 15% of the entire dataset. The authors carried out a sensitivity analysis over the adopted explanatory variables
149 (distance from edge of the road, light and heavy-duty vehicle volume and composition, average speed, roadway
150 temperature) to shed some light on the black-box paradigm of the neural network. In [40] V. Nourani et al.
151 presented the first application of the Emotional ANN (EANN) as a new generation of neural network methods
152 for predicting the equivalent noise level $L_{eq,15'}$ from road traffic noise in Nicosia. The traffic volume was
153 found to be the most significant contributing factor whereas heavy-vehicle volume was found to be the least
154 (in accordance with the study [38] mentioned above). No information is provided about the composition of the
155 training, validation, and test sets.
156 P. Kumar et al in [41] trained a multilayer feed forward BP neural network by using the Levenberg–
157 Marquardt algorithm for predicting highway traffic noise in an Indian scenario. A location characterized by
158 free-flowing-traffic conditions, avoiding sources of interruptions, was selected omitting nighttime traffic
159 volumes from the predictions. The proposed ANN model was used to predict 10 percentile levels (L_{10}) and the
160 equivalent continuous sound level in dB(A) using as source of input data the average hourly values of the
161 traffic flow. A Comparison between regression analysis and experimental values revealed a percentage training
162 error ranging from -4.2 to 2.7 for L_{10} and from −5.1 to 2.6 for L_{eq}, while for the test samples the error is within
163 the range −4.1% to -0.1% for L_{10} and −4.8% to 0.5% for L_{eq}. The ANN model outperformed the regression
164 analysis. Indeed, the training error of the ANN model lies within the range -0.8% - 1.0% for L_{10} and −1.5% -
165 0.9% for L_{eq}, while for testing samples the error ranges from −1.7% to 1.8 for L_{10} and from -0.6% to 1.5% for
166 L_{eq}. The training and test set sizes were 80% and 20% respectively of the whole dataset composed of 46 hourly
167 records.
168 In [30] V. Nourani et al. adopted an original ensemble approach for combining the response of four
169 different models aimed to improve traffic noise prediction performance in Nicosia. Three AI-based models
170 (fuzzy, neural network, support vector regression algorithm) were employed while the fourth was based on a
171 conventional multilinear regression model. Measurements were performed during daytime (omitting
172 nighttime) at observation points carefully selected for avoiding as much spurious background noise as possible.
173 The ensembled model was then used to predict the equivalent sound level L_{eq}, considering 15 minutes
174 integration time and using traffic composition and average vehicle speed as input data..
175 L. Chen in [42] developed a neural network model for traffic noise prediction in a mountainous city. A
176 multilayer feedforward ANN model was trained using experimental data measured in a municipal road in a
177 hilly Chinese city (Chongqing). Measurements were performed, at observation points carefully selected for
178 operating under free-flowing traffic conditions. The proposed ANN model was used to predict the per-vehicle
179 noise levels and the corresponding equivalent sound level pressure. Comparison between the neural model and
180 the Chinese standard HJ 2.4-2009 revealed a significant improvement over the empirical equations.

In [43] S. Givargis et al. presented a basic Multi-Layer Perceptron (MLP) model for predicting hourly equivalent sound pressure levels. The authors conducted a comparison with the CORTN model in order to investigate whether a neural network can be used in a statistical manner to model traffic noise for Tehran's roads. The result of the study revealed the ability of the MLP model to provide a description of the traffic noise consistent with the conventional statistical approach of the CORTN model.

In [44] D. Singh et al investigated using four different soft computing methods, (generalized linear model, decision trees, random forests, and neural networks), for predicting continuous hourly L_{eq} at different free-flow traffic location locations in an Indian city. The Random Forests method outperformed the other approaches in predicting the sound pressure level.

1.2 Short-term traffic noise prediction in waterfront of seaport cities.

From the above overview, an exiguous number of studies emerges that have probed in developing dynamic models for traffic noise prediction in complex urban contexts where actual traffic conditions cannot be properly described by a priori and restrictive assumptions on traffic behavior and background noise. Continuous traffic flow regime or general features drawn from regular scenarios even under unperturbed boundary conditions, are, in some cases, unrealistic assumptions that do not adequately account for the acoustic field in response to the short - term evolution of traffic sources and under real operating conditions.

The motivation of the present work stems from the following consideration. Several waterfront cities experience through traffic of private and commercial vehicles attracted by port activities, especially in tourist destinations. During the peak season the soundscape of an urban waterfront in port cities undergoes substantial changes throughout the day and night on an hourly or sub-hourly time scale that however is not always univocally and a priori predictable. This phenomenon is caused by the ferry traffic which tangibly has a direct impact on the vehicle flows through the road network in urban waterfronts in port cities. Exposure to noise in urban port waterfront areas takes on a different connotation compared to other urban contexts, particularly in those cities with commercial ports strongly impacted by the seasonality of tourism demand. The concentration of ferry departures and arrivals, during the peak season, generates a large amount of tourist with an exceptional intensification of the vehicular and heavy lorry traffic (in comparison with the average yearly trend), conditioning driving strategies and behavior, especially when drivers have to comply with boarding times.

This phenomenon occurs with an unpredictable and variable time scale during days of the peak tourist season and culminates every weekend. In the case at hand, the traffic flow can increase by about (730-1000)%. The consequences on the acoustic pressure generated by vehicle engines are easy to imagine. Therefore, the presence of an urban port exposes the neighbouring areas to a wide range of temporal variation in traffic volumes, potentially creating complex constantly evolving acoustical scenarios [45]. Certain buildings may thus be subject to annoying traffic noise, as low levels in normal times alternate with heavy traffic volumes on road connections to the port. Changes in vehicular flow intensity and composition occur during boarding and disembarking. Exceptional increases in traffic flows during port operations negatively impact the livability of

the waterfront areas as well as the tourist appeal of the city as a whole. Thus, the waterfront area is solely perceived as a thoroughfare for reaching quieter places.

Static traffic–noise models, based on purely statistical assumptions, or even dynamic models operating with a time refinement of an hour or longer are not able to satisfactorily incorporate and reproduce the dynamic features in similar acoustical contexts with the proper time scale and accuracy.

Therefore, similar approaches could lead to unrealistic results in predicting the impact of traffic management strategies aimed at reducing urban noise.

From the foregoing discussion, it would be advisable that a traffic noise prediction model, designed to identify a series of predefined traffic management strategies and to combat the uncontrolled evolution of the traffic noise levels in urban waterfronts, needed to be dynamic, accurate and to operate in real time with the actual traffic conditions at time scales smaller than the considered acoustic phenomenon. Analysis of the pertinent literature showed that a full transient dynamic model that predicts the equivalent noise level, from the traffic flow, with a small prediction error (lower than 1 dB) and a small-time refinement (1 minute), is not yet available.

Consistent with this overarching objective, we addressed the problem of identifying a dynamic model that was able to replicate, or at least approximate, the data generation mechanism by means of which the flow and composition of vehicle traffic produces noise levels in a specific urban context. Therefore, we implemented a dynamic prediction model architecture with exogenous inputs that dynamically predicts noise level trends, with a short time refinement and a small prediction error, as the noise sources, arranged in different traffic scenarios, vary.

An adaptive nonlinear autoregressive recurrent dynamic neural network model has been developed, trained, and experimentally tested for the short-term prediction of the equivalent noise level $L_{eq,1'}$ generated by vehicular traffic in the port city of Olbia chosen for the case study. Olbia, a medium sized city on the Mediterranean Sea exhibits the peculiar characteristics of a port city with seasonal variations in traffic volumes, due to the major tourism flows attracted by the port. Once the area of interest was suitably scaled down to be more appropriate with the research objectives, the exploratory analysis focused on the area affected by direction of the traffic traveling to the Isola Bianca quay for freight and passenger loading and unloading operations.

The neural model simultaneously predicts the experimental sequence of the time averaged equivalent sound pressure level $L_{eq,1'}(\tau)$ of the traffic noise at three different locations, representative of the acoustic field in the waterfront line: i) a signalized intersection, ii) a roundabout, and iii) the entrance to a vehicular underpass.

The three locations exhibit a wide variability and different traffic conditions and were selected for the significant correlation between vehicular traffic and port activities, observed during preliminary monitoring carried out over a period of several years prior to the present study.

The architecture adopted for developing the model belongs to the so called NARX models [46] and is nonlinear, autoregressive and accepts exogenous input and feedback regressors as source of input data. The

intensity and the composition of the traffic flows have been used as exogenous inputs, while regressors of the acoustic output have been employed as feedback input.

Moreover, the model is based on a restricted number of experimental observations of the traffic noise event, circumventing the need for a preliminary data collection stage for incorporating all possible occurrence of the traffic noise phenomenon.

Indeed, this type of prediction system is employed for its ability to generalize the results and hence to associate correct responses even to input signals not previously contemplated or with missing or partially missing information. The prediction capability of the NARX model is demonstrated over a 6-day time span measured in two distinct periods of the year: for normal and peak traffic conditions.

The neural model, once has been trained, is able to operate in multi-step head prediction mode. The time required for provide predictions with a time refinement of 1 minute is less of 14 [ms]. Therefore, the developed model operates in real time mode, with respect to the considered time frame of 1 minute. These features offer potential for supporting the decision processes in traffic management with short- term refinement where the ability to predict the effects of different traffic strategies can be very useful

2. Description of the measuring periods and selection of the measuring points and methods.

Fig. 2 shows a satellite image of the urban area of the Olbia's waterfront indicating the distribution of the traffic sensors and three sound pressure meters are schematically reported. A roundabout, a signalized intersection, and a wide entrance to a vehicular underpass, the most exposed area to traffic volume generated by port activities, mark the imaginary line of the waterfront city and have been acoustically monitored during the measuring periods being. The distribution of the road sections was decided on the basis of our intention to monitor all those sections along the preferential routes in and out of the port and that provide access to the city's waterfront. In addition, we considered sources of traffic congestion such as the signalized intersections and roundabouts along the port waterfront (see measurement points A e B shown in Fig. 2).

A total of 11 road sections were continuously monitored, as shown in Fig. 2. Note that four road sections are two-way roads (sections 1, 9, 10, and 11), while the remaining 7 are one-way streets (2, 3, 4, 5, 6, 7, and 8), making a total of 15 road lanes.

The representativity of the selected points was confirmed by preliminary noise level measurements in both periods that in a first approximation showed a close correlation of the traffic volume fluctuations with the corresponding variations in noise levels.

The area is a popular tourist destination with marked seasonal variations. Indeed, the volume and composition of traffic along the city's waterfront can be divided into two very different periods. The first is the normal (off-season) period, $T_{\text{off-s}}$, from October to May where traffic volumes are mainly generated by the daily routine of the residents and by ordinariness of production activities. The second is the peak period, $T_{\text{pk-s}}$, that goes from June to September where traffic volumes increase substantially by comparison with the average yearly trend because of the large number of tourists arriving at and departing from the port. During these

months vehicle traffic increases substantially by about 730 – 1000%, culminating in the third weekend in August.

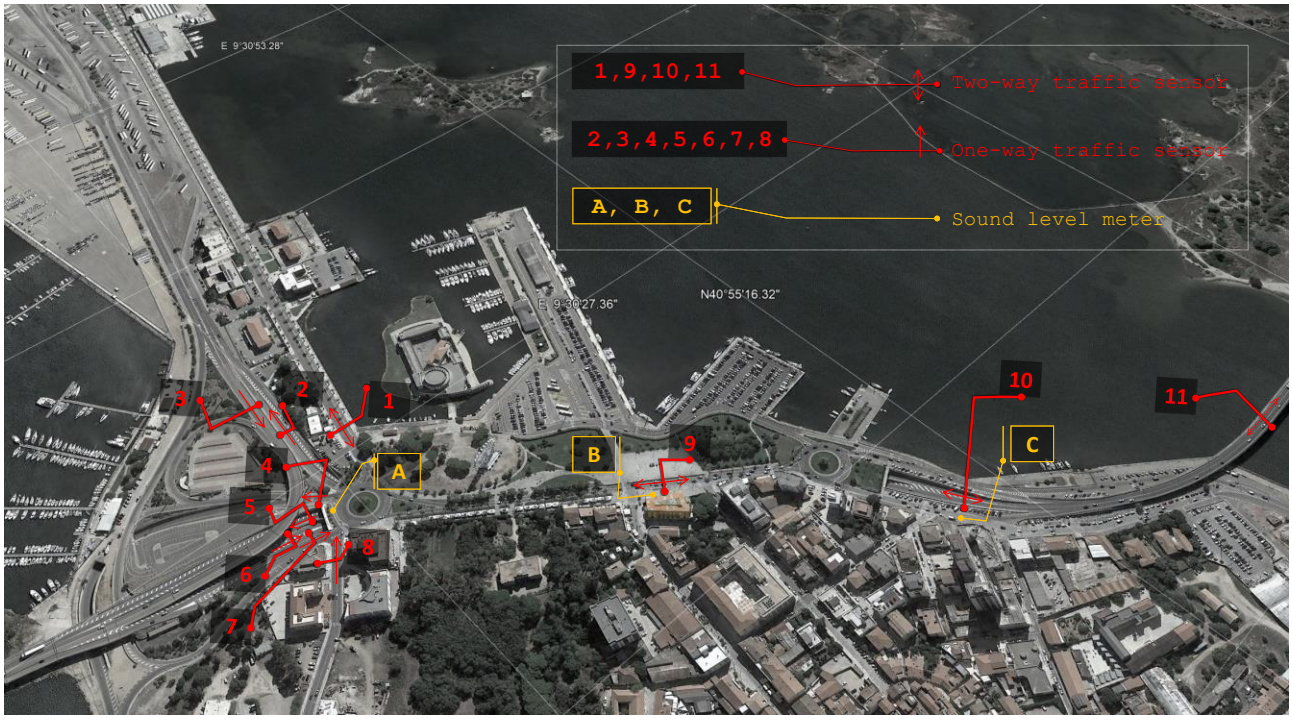

Fig. 2. Monitoring area of the Olbia waterfront. Optimized selection of vehicle traffic measurement points (red) and sound pressure level meters (yellow).

Fig. 3 Local contextualization of the measurement points. a) position of the sound level meter at the "Principe Umberto" roundabout denoted with A in Fig. 2; b) position of the sound level meter at the signalized intersection in front of Olbia town hall, denoted with B in Fig. 2; c) position of the sound level meter at the entrance to the underpass denoted with C in Fig. 2. d) position of the traffic sensor number 4 in Fig. 2. e) example of traffic flows along the waterfront during daytime; f) example of traffic flows along the waterfront at nighttime at sound level meter A.

In the present investigation noise level and traffic data measurements were performed in two continuous periods each of 72 hours duration. During each period the temporal evolution of sound pressure levels $L_{eq,1'}$ was acquired simultaneously with the traffic data (category, traffic volume and speed of the vehicles) in fifteen sections of different road lanes. The first between March 24th 27th, representative of the off-season period characterized by normal traffic volumes, the second between August 24th and 27th representative of the peak season.

The choice of measurement points fell on those locations that were able to provide a sufficiently complete and representative picture of noise levels in the port area.

3. Neural network architecture

The traffic – noise model has been implemented adopting the architecture of a nonlinear autoregressive exogenous (NARX) artificial neural network in a closed loop configuration [47]. The reason for adopting a NARX architecture relies on its specific suitability for implementing time series prediction tasks where external independent physical input affects the behavior of the output time series to be predicted, with the contribution of its past values.

This kind of autoregressive architecture can adapt its parameters on the past values of the output sequence and in addition other exogenous inputs are accounted for as driver of the future values by specific input nodes.

This means that the NARX model relates the history of the time series to be used as feedback input, with the current and past values of other external independent explanatory inputs by a using a learning algorithm that drives adaptation of its parameters for reproposing the temporal relationship between inputs and output observations.

The training of the network parameters takes place for each value of the sample of the input sequence that is supplied to the network. At every training step the Levenberg-Marquardt back-propagation optimization scheme is applied for reducing as much as possible the overall error between the answer given by the network at the actual instant, with respect to the relative target, and the error of the answer given at a certain number of preceding instants.

The NARX model could be utilized to solve time series prediction problem where the task consists in predicting future values of a given time series $\ell(\tau)$ from its past values and from past values of another time series $\mathcal{s}(\tau)$. The past values of the time series $\ell(\tau)$ represents endogenous input, while the values of the second time series $\mathcal{s}(\tau)$ represents the exogenous-input. This form of prediction can be represented by the following describing equation:

$$\ell(\tau) = \mathcal{F}(\ell(\tau-1), \dots, \ell(\tau-r_n), \varepsilon(\tau), \dots, \varepsilon(\tau-r_t)\ ) \quad \text{Eq. 1}$$

where $\ell(\tau)$ corresponds to the next value of the output to be predicted at instant τ and by means the function $\mathcal{F}(\ \ )$ is regressed on previous values of the output signal, $\ell(\tau-i)|_{i=1\dots r_n}$, and previous values of the independent exogenous input quantity, $\varepsilon(\tau-j)|_{j=1\dots r_t}$.

The traffic noise model can be implemented on the NARX architecture by assuming the following correspondence: the time profile of the equivalent noise level $L_{eq,1'}$, obtained by averaging over an integration time of 1 minute, plays the role of dependent variable in place of the output signal ℓ in Eq. 1. In particular $L_{eq,1'}(\tau)$ represents the output value to predict at instant τ, while $L_{eq,1'}(\tau - i)\big|_{i=1\dots r_n}$ represent the past values of the noise level that have to be used as regressors for predicting the next values of $L_{eq,1'}$. The time profiles of the traffic flows data $[\mathcal{traffic}(\tau)]$, averaged over 1 minute play the role of independent variable in place of the exogenous input signal ε in Eq. 1. Clearly, the traffic flow data variable $[\mathcal{traffic}(\tau)]$ is not simply composed by a scalar time sequence, like $L_{eq,1'}$, but incorporates the time sequences $\dot{V}(\tau)$, $v(\tau)$ describing the temporal evolution of the flow rates and the speed for each vehicle class and each lane that composes the road sections, under consideration.

The NARX model can be implemented by means a neural network that provides an approximation of the mathematical expression of the function $\mathcal{F}$. The input data source is composed of the regressor values of the acoustic pressure level $L_{eq,1'}$ of the noise signal (in feedback or open loop arrangement) and of the parameters describing traffic composition and road layout. The NARX model should be trained using input values at instant τ_i and the values occurring at past instants τ_{i-1}, τ_{i-2} and τ_{i-n} so that the model is able to learn not only the individual measured values but also the temporal dynamics with which they occur.

It is worthwhile to introduce Fig. 4 since it provides insight into the architecture of the resulting NARX model. The schemes of Fig. 4a and 4b represent a two-layer feedforward neural network, with a sigmoid transfer function in the hidden layer (to treat nonlinear separable solutions) and a linear transfer function in the output layer. In both schemes, the networks are equipped with tapped delay buffers to store past values of $L_{eq,1'}(\tau)$ and $[\mathcal{traffic}(\tau)]$ sequences. In Fig 4a the network exhibits a close loop configuration, where the output of the network is fed back as source of input data for implementing the instantaneous dependence of $L_{eq,1'}(\tau)$ from its past values $L_{eq,1'}(\tau - i)\big|_{i=1\dots r_n}$. In this case the regressors are numerically calculated by the network algorithm and derived from its output. Therefore, they are estimated values. In Fig. 4b an architecture in open loop configuration is depicted where the regressors of $L_{eq,1'}$ are directly extracted from the experimental observations. The open loop configuration should be used during the training phase of the network, since the exact output values are available from measurements, rather than feeding back the estimated output. Thereby, the network can adapt its parameters on input values that are measured and then more accurate than the estimated values achieved with the closed loop configuration.

Moreover, the training procedure can be performed by means a more efficient algorithm if a feedforward architecture is adopted in place of a feedback nework.

Once the training stage of the network has been carried out in open loop configuration, by utilizing the scheme illustrated in Fig. 4b, the typical workflow includes a further step in which the trained network is transformed in closed loop configuration (according to the scheme of fig. 4a) for generating multistep-ahead predictions.

The model has been built using Matlab development environment that allows to display the autocorrelation function of the prediction and the input -error cross-correlation functions that describe how the prediction errors are related in time with each other and with the input respectively. The adequacy of an identification model to the experimental observation is, in some extent, revealed by behaviour of the autocorrelation and cross-correlation function in so far as they approach to zero values throughout the lag abscissa, except in the origin at zero lag value where the function should attain its maximum value for the case of the autocorrelation function. These conditions would denote that the prediction errors are weakly or completely uncorrelated with each other and with the input sequence. If there is no dependence among these residuals, then they can be regarded as observations of independent random variables (white noise), and there is no further modelling to be done except to estimate their mean and variance. However, if instead there is significant dependence among and between the prediction error values and input sequences then it should be possible to improve the predictions by looking for a more complex time series model, for example by adding hidden layers, that accounts for the showed dependence, or perhaps by increasing the number of delays in the tapped delay lines. This could be beneficial, since dependence aspect may imply that past observations of the noise sequence can assist in predicting future values. Therefore, the autocorrelation and cross correlation function can help for assessing the proper complexity of the network and the size of the regression vectors that exhibit to improve the adequacy of the trained model to the observed data generation mechanism.

Specifically, in the present study the hidden layer size and the number of the input and feedback regressor has been found by tuning them (throughout a trial-and-error technique) until no further improvements on the prediction error and the auto and cross - correlation functions were revealed. As a result, the number of the regressor considered for the training phase is 1 for the traffic flow data and 3 for the level noise data. The choice has been also validated by the Lipschitz Quotients criterion proposed for the first time by He and Asada (1993), and later developed by Jeen- Shing Wang et al. (2009), for dynamic neural models of the MISO (Multi Input Single Output) type.

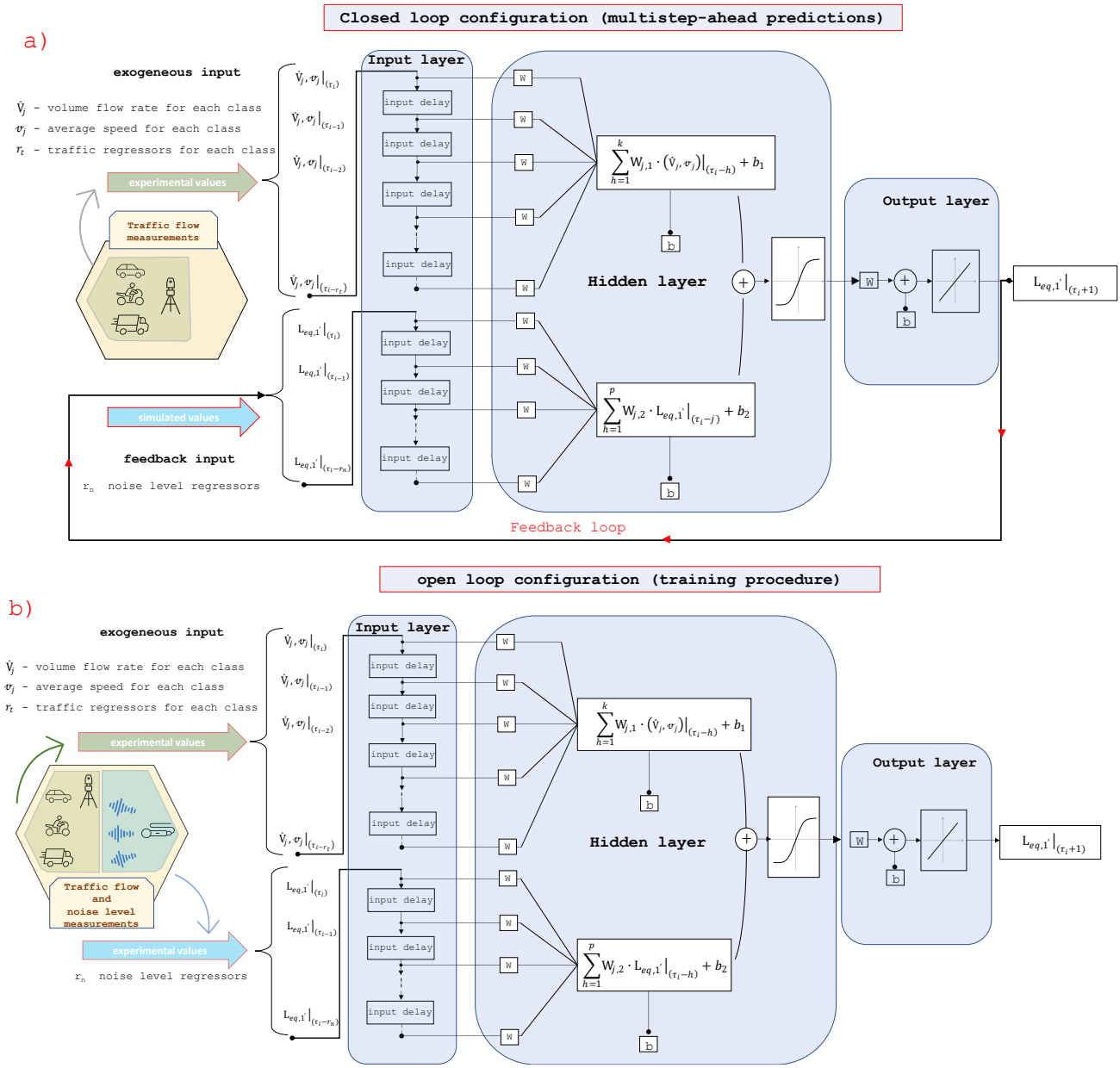

Fig. 4 Schematic representation of the architecture of the adopted NARX model. a) closed loop configuration for multistep-ahead prediction. In this configuration the trained model is driven by the traffic flow measurements for predicting the noise level. The simulated noise levels at previous steps are fed back as source of input data for implementing the temporal dependence of $L_{eq,1'}(\tau)$ from its past values. b) open loop configuration for performing the training stage. The values of the traffic flow, the noise level and their regressors are extracted from the experimental observations and are used as source of input data.

The experimental observations are composed by 8640 records of noise level measurements and an equal number of traffic noise data. Half of these concerns the time series measured during off-season traffic volumes, while the other half refers to the peak traffic season. The learning algorithm is based on the Levenberg-Marquardt back-propagation optimization scheme applied for least-squares estimation of nonlinear parameters [48 - 49]. At each training step the algorithm reduces the overall error between the response provided by the network and the corresponding experimental value representing the correct target. For the benefit of the reader, an overview of the sources and the

420 structure of the input and output data, supplied to the model for developing the training and testing
421 procedure, are reported in the following scheme.
422

source of the exogenous input data	experimental values of the traffic flow data sequence, ($[t\!\!\not\!\!d(\tau)]$): a) traffic flow rate, in terms of the overall number of vehicles per unit time (1 minute) crossing a reference section of a given roadway, $\dot{V}$. b) average value of the different speeds of a class of vehicles measured at a given point by the traffic sensor during a time of 1 minute, v. The traffic flow rate $\dot{V}$ and the average speed v are separately provided for each vehicle's category, as defined accordingly to the CNOSSOS-EU standard and for each lane that composes the roadways under consideration. Separate quantities for each lane allow to incorporate the information about the driven direction in the training processes.
n° of monitored roadway sections	11 measuring points placed as shown in Fig. 2. Four road sections are two-way roads (sections 1, 9, 10, and 11), while the remaining seven (2, 3, 4, 5, 6, 7, 8) are one-way streets, making a total of 15 road lanes
n° of vehicle's categories	vehicles are grouped into four categories on the basis of their emission characteristics as defined in the Common Noise Assessment methods (CNOSSOS). Specifically: a) light motor vehicles, b) medium heavy motor vehicles, c) heavy vehicles, d) powered two wheelers (motorcycles and moped). In the case of powered two-wheelers (category 4), two subclasses had to be defined: a class 4a for mopeds and a class 4b for more powerful motorcycles, since they have very different driving modes, and their numbers usually vary widely (as indeed happens between the off-season and peak traffic periods due to the large number of tourists arriving at and departing from the port).
n° of exogenous input	75 exogenous inputs, resulting from the combination between the number of roadway lanes and the number of the vehicular classes. In particular, 5 vehicular classes (considering the two subclasses 4a and 4b) for 15 roadway lanes. Each datum contains two pieces of information collected for a time period of 1 minute: the average vehicle speed, v and the flow rate, $\dot{V}$.
source of the output target data	experimental values of the equivalent noise pressure level $L_{eq,1'}(\tau_i)$ sequence obtained by averaging over an integration time of 60 seconds.
n° of acoustic measuring points	3 measuring points placed as shown in Fig. 2.
n° of output	3 noise level outputs.
source of the feedback input (regressors)	past values of the noise level and traffic flow sequences, namely $L_{eq,1'}(\tau - i)\big\vert_{i=1\ldots r_n}$, $\dot{V}(\tau - j)\big\vert_{j=1\ldots r_t}$ and $s(\tau - j)\vert_{j=1\ldots r_t}$.
size of the feedback regressors	r_t = 1 traffic data regressor. r_n = 3 noise level data regressors.
n° of hidden layers	4 hidden layers.
n° of measurement periods	two continuous periods each of 72 hours duration. 1st period, $T_{\text{off}-\text{s}}$, that covers March 24th and 27th, representative of the off-season period of the traffic flow rate. 2nd period, $T_{\text{pk-s}}$, during August 24th and 27th, representative of the peak season period of the traffic flow rate.
time refinement	T_r = 60 seconds.
n° of records of input/output sequences	8640 records each averaged over a time span equal to T_r. Specifically 4320 records are measured during $T_{\text{off-s}}$ period and other 4320 during $T_{\text{pk-s}}$ period.
input and target training sequences size	800 ÷ 950 records of $L_{eq,1'}(\tau)$ and $[t\!\!\not\!\!d(\tau)]$ sequences, extracted from the $T_{\text{off}-\text{s}}$ period.

input and target test sequences size	7840 ÷ 7680 records of $L_{eq,1'}(\tau)$ and $[\not{t}\not{d}(\tau)]$sequences, measured during the $T_{\text{off-s}}$ and $T_{\text{pk-s}}$ periods. In particular 3520 ÷ 3350 records come from the remaining part of $T_{\text{off-s}}$, that is omitted by the training procedure and other 4320 records are provided by the whole $T_{\text{pk-s}}$ period.

3.1 Input and output data sets

The neural model accepts an $m \times n$ matrix, containing all the traffic composition information, as source of exogenous input [I]. Two explanatory variables are used for characterizing the traffic on each road lane and for each vehicle class: a) the number of vehicles per minute and the average speed for each class. The row index j $(1..m)$ selects the explanatory variable of a given road lane and vehicle category while the column index k $(1..n)$ goes through the temporal samples, obtained by averaging the physical sample with a refinement of one minute. The value of the row index m is equal to the number of explanatory variables, (2) multiplied by the number of road lanes monitored (15) and by the number of the vehicular categories (5), therefore $m = 15 * 2 * 5 = 150$, while the value of the column index n is equal to the total number of temporal samples, namely $n = 8640$.

The neural model returns the $q \times n$ target matrix [T] as output. The output matrix contains the temporal evolution of the noise level at the given measurement points. The value of the row index is equal to 3, the same as the number of noise level measurement points.

The training and the testing processes take as neural model input and output the submatrices extracted from $[I]$ and $[T]$ respectively.

4. Training Procedure

The success of the neural network approach relies on a preliminary phase, termed the *training process*. During this step the network adapts its parameters in order to learn the information contained in the *training set* data.

Throughout this preliminary training process, at each training step the experimental noise level at a given instant is a known target and is used by the internal algorithm to iteratively adjust the network parameters to minimize the overall error between the right experimental targets and the simulated response of the network.

The preliminary training process was carried out on a temporal sequence of traffic-noise data containing 800 and 950 records corresponding to 9% and 11% respectively of all the experimental observations (depending on which measurement point A, B or C was considered). The training sequence covers a period ranging from nighttime to early morning and is characterized by a wide transitoriness of the traffic conditions.

The remaining sequence, ten times larger than the training sequence, containing 7840 or 7680 records corresponding to 91% - 89% respectively of the experimental observations were used for validating the generalization stage.

Figures 5 and 6 show the sound pressure level evolution, during the off-season measurement period (24-27th March 2019) at the measurement point situated in position A (indicated in Fig. 2). Two schemes of

training strategies throughout the classical dynamics alternating between daytime, evening, and nighttime are shown. Two different strategies have been devised: a single and a multiple time span. They were both implemented but for brevity only the results of the single time span are reported here as this strategy performed better.

The multiple time span strategy consists in identifying a certain number *h* of intervals, evenly spaced along the timeline in an attempt to capture the dynamics of the noise event in each segment. Figure 5 gives an intuitive picture of how this strategy splits the time - line into training and test set intervals. However, this strategy did not produce the expected results. Though the training set comprised a number of intervals spread over the measurement period, each segment was not sufficiently long to identify the relationship between traffic and noise data in transient conditions. The results presented in the next sections, obtained adopting the single time span training strategy, show that it outperforms the interleaved multiple short -time spans having the same overall size as the single one.

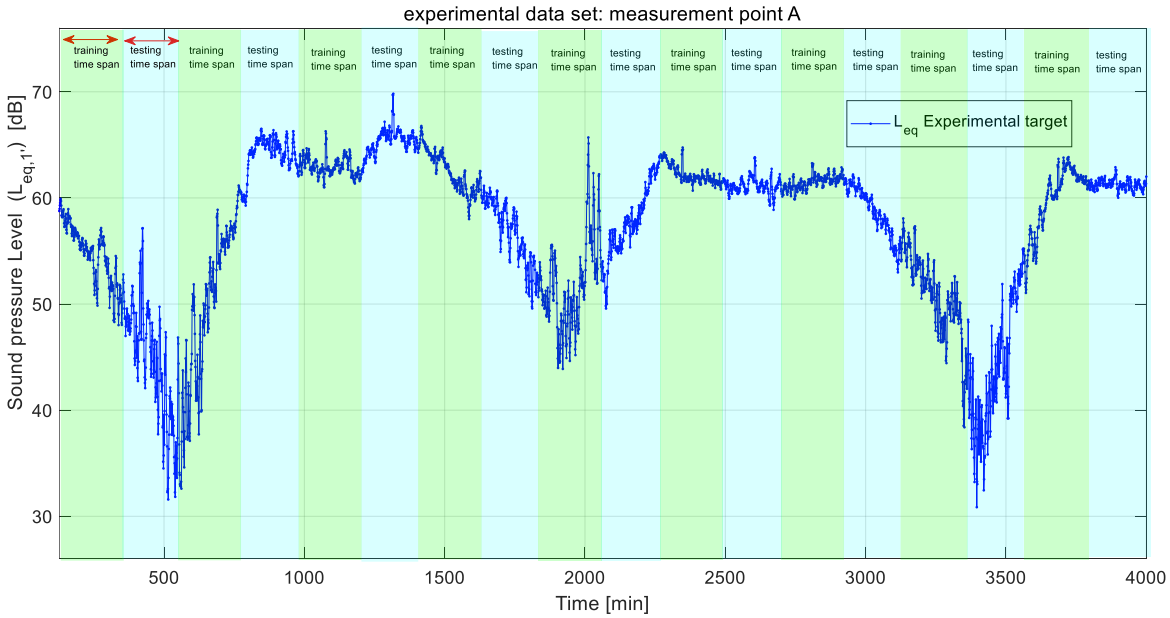

Fig. 5. Sound pressure levels vs. time, during off-season measurement period in position A, showing the periods to which, the data considered for the training and test sets, obtained using an interleaved multiple time spans learning scheme, refer.

The other strategy consists in extracting a single continuous time span from the measurement period, of sufficient duration to ensure that traffic composition and noise levels exhibit a transient response. This single interval is employed for training, while the remainder of the measurement period is used for the subsequent test phase. Figure 6 gives an intuitive picture of how the single time span scheme selects the training set from the complete timeline.

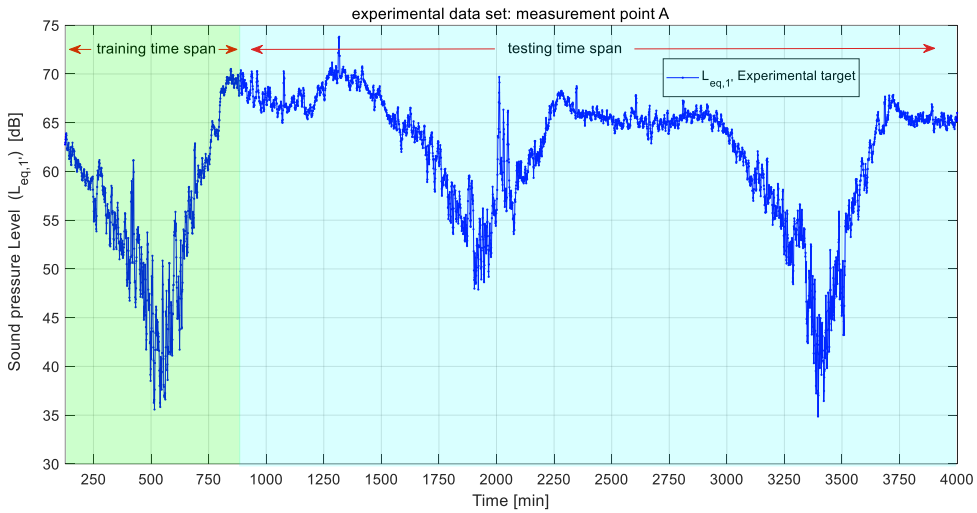

Fig. 6 Traffic noise measurements showing the periods to which the data considered for the training and test sets, obtained using the single time span strategy, refer.

Figure 7 summarizes the results obtained. The continuous time interval comprises both day- and nighttime periods. As can be seen, the network has been trained within a time span in which the acoustic time-series exhibits a transient trend.

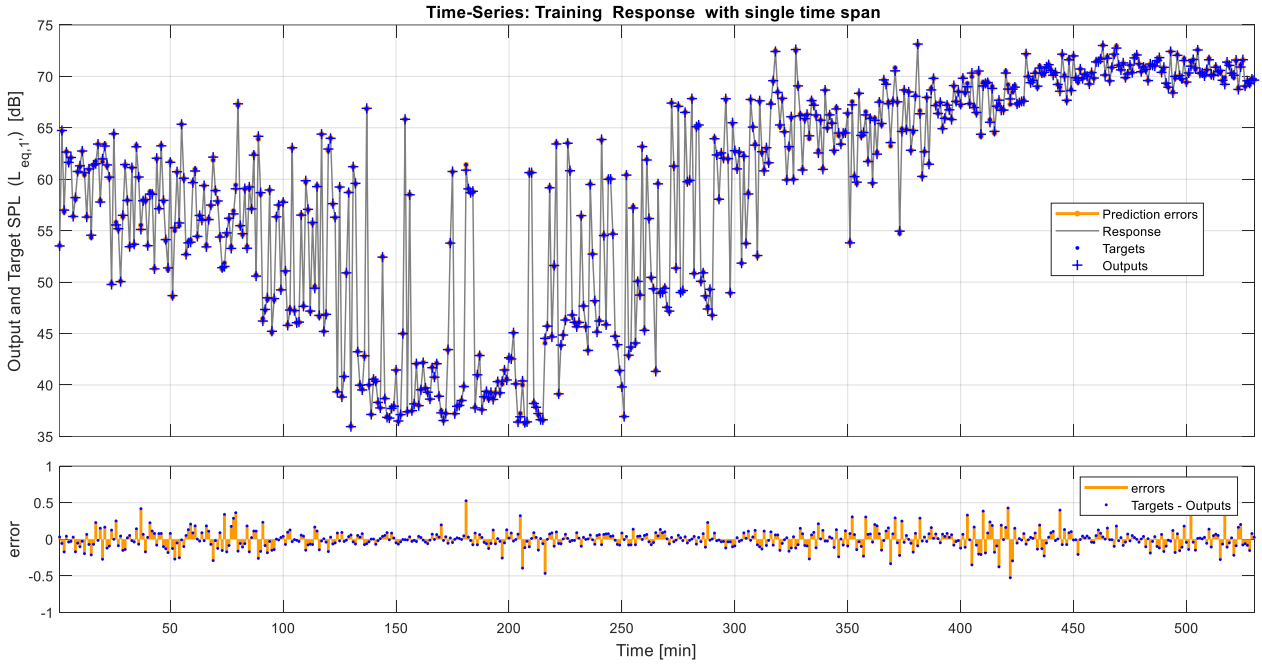

Fig 7. Example of training response using the single time span strategy. Time span of 550 minutes with a time refinement of 1 sample/min

5. Results of the training and test processes.

Once the training process is completed using the experimental data entered into the submatrices $[I]_{\{m,v\}}$, $[T]_{\{q,v\}}$, the internal parameters of the network are numerically determined and thus take constant values. The

493 model is now potentially ready for performing prediction tasks over the entire measurement period. Therefore,
494 the next step consists in testing the learning rate achieved by the network during the previous step, since it is
495 quite desirable the ability to predict the right sequences of $L_{eq,1'}(\tau_j)$, omitted from the training process, that
496 cannot have any effect on the training stage. Indeed, the correct prediction of noise levels, generated at a given
497 point for any profile of the traffic flow, dominates the developing process of a simulation model.

498

499 *5.1 Training process*

500 In this section the relevant results of the training processes of the NARX model by applying the
501 measurements performed during the *off-season traffic condition*, are reported.
502 In Figs. 8, 9 and 10 the simulated response of the model $L_{eq,1',sim}$ is compared with respect to the experimental
503 target $L_{eq,1',exp}$ for vehicle traffic data completely extracted from the training set. The prediction errors are
504 shown in specific subplots.
505 Figures 8, 9 and 10 show the figures of merit describing the reliability and effectiveness of the NARX
506 model identified for each measurement point as a result of the training process response.
507 In Figs. 8a, 10a and 12a the simulated and experimental values of $L_{eq,1'}$ measured at points A, B and C
508 are compared, while the prediction errors are shown in specific subplots.
509 In Figures 8b, 9b and 10b the regression function of the input and output data is reported. The cluster of
510 points around the straight-line bisector indicates better performance. The closer the regression coefficient R is
511 to 1, the better the regression of the values estimated by the neural network with respect to the experimental
512 data.
513 Figures 8c, 9c and 10c show the autocorrelation of the prediction error function. It describes how the prediction
514 errors are related in time. A well performing prediction model requires a single non-zero value of the
515 autocorrelation function at zero lag, whereas for lag times different from zero, it should be close to zero. This
516 requirement represents a no-correlation condition throughout the prediction errors.
517 In Figs. 8d, 9d and 10d the cross - correlation function of the prediction error and the exogenous input
518 sequence is shown. The cross - correlation function provides a picture of how the errors are correlated with the
519 input traffic composition sequence. For a perfect prediction model, the correlations should be close to zero
520 across the entire lag domain.
521 The auto and cross correlation functions are a figure of merit to consider when assessing whether and to
522 what extent the identified model can explain the functional interdependence of the experimental observations.
523

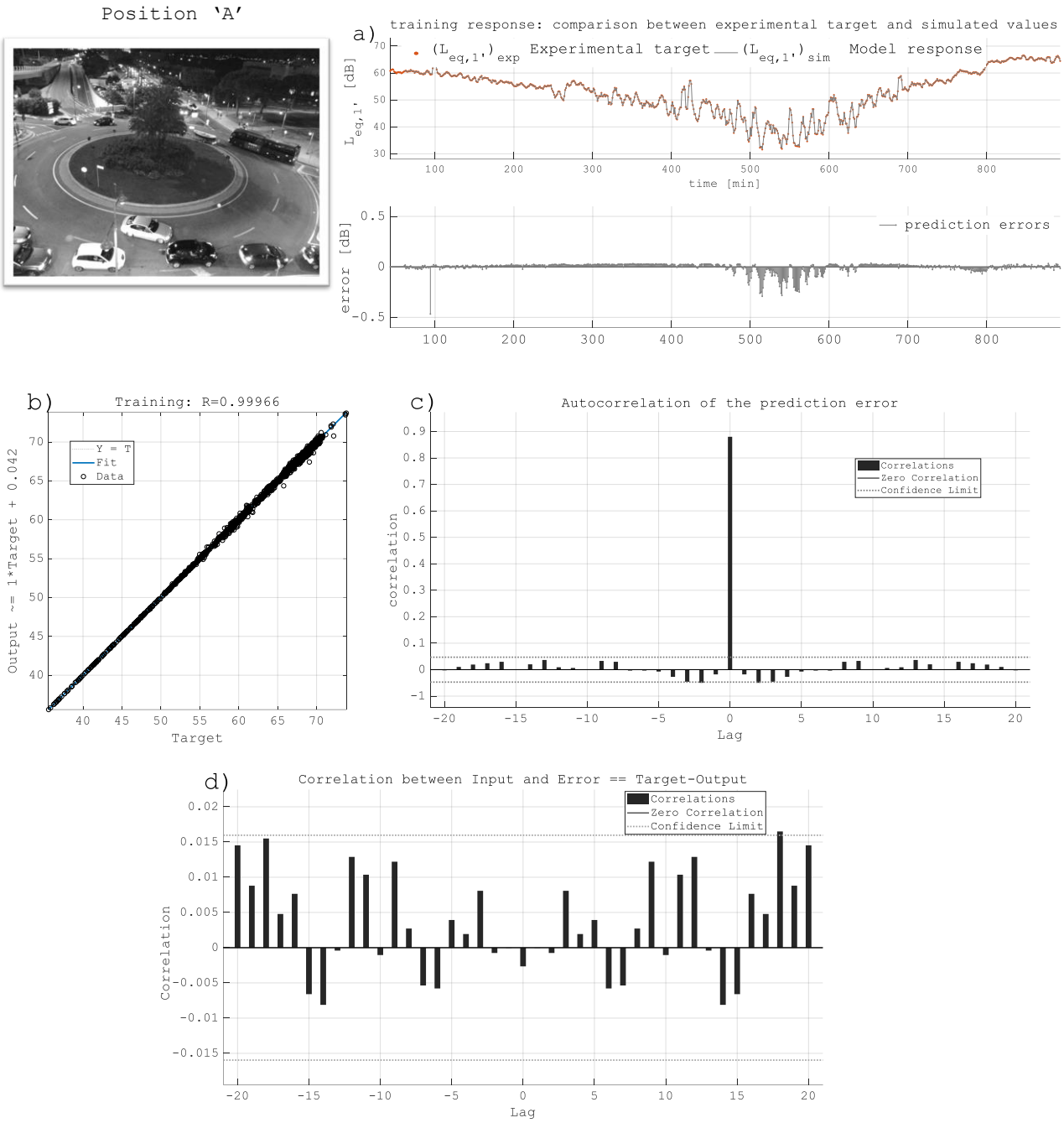

Fig. 8 Training performances for experimental data measured at point A. In a) comparison and prediction error of simulated and measured $L_{A,eq,1'}$; b) regression between traffic input and acoustic output sequences; c) autocorrelation function of the prediction error sequence. d) cross-correlation function between prediction error and traffic input sequence.

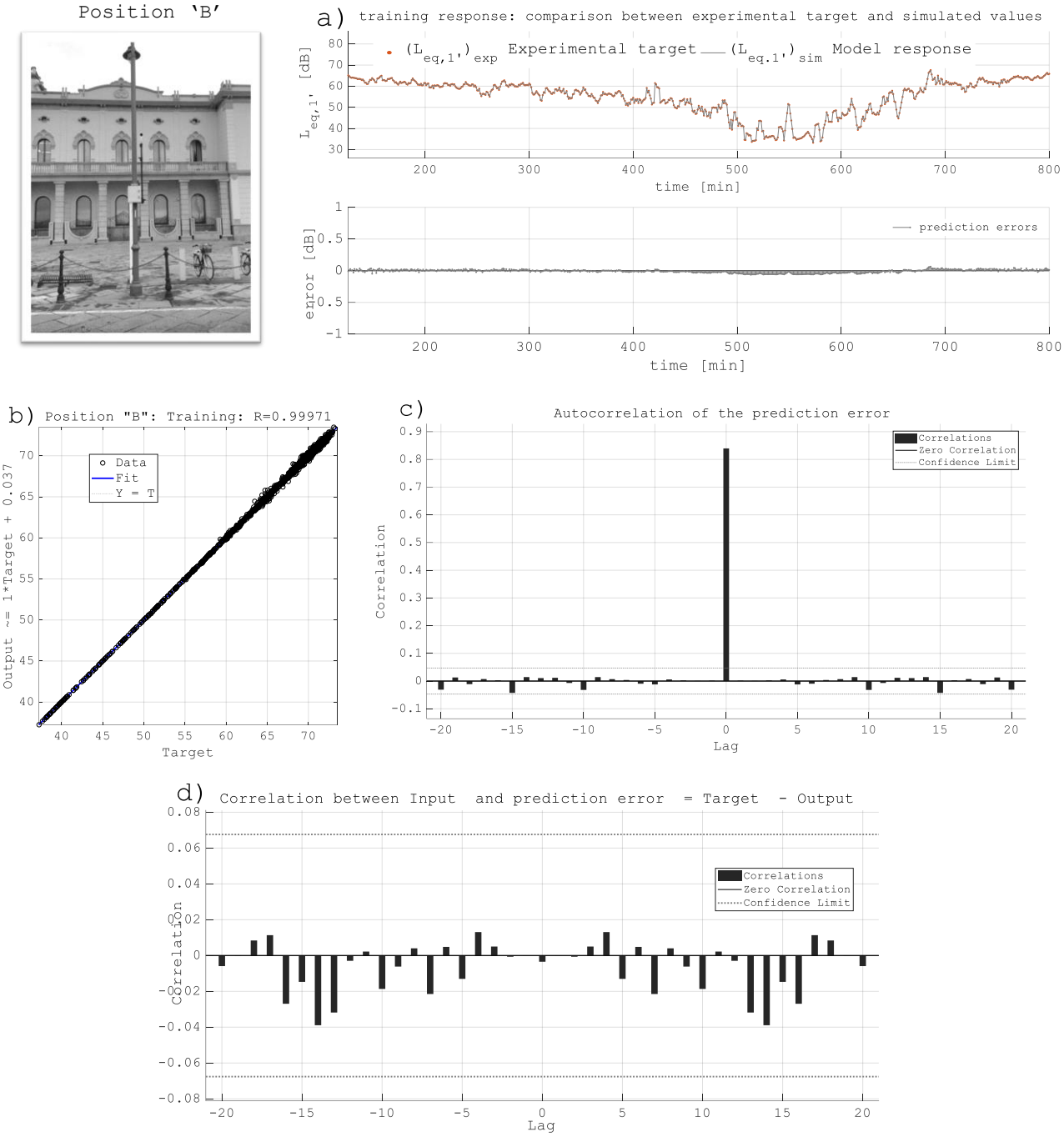

Fig. 9 Training performances for experimental data measured at point B. In a) comparison and prediction error of simulated and measured $L_{A,eq,1'}$; b) regression between traffic input and acoustic output sequences; c) autocorrelation function of the prediction error sequence. d) cross-correlation function between prediction error and traffic input sequence.

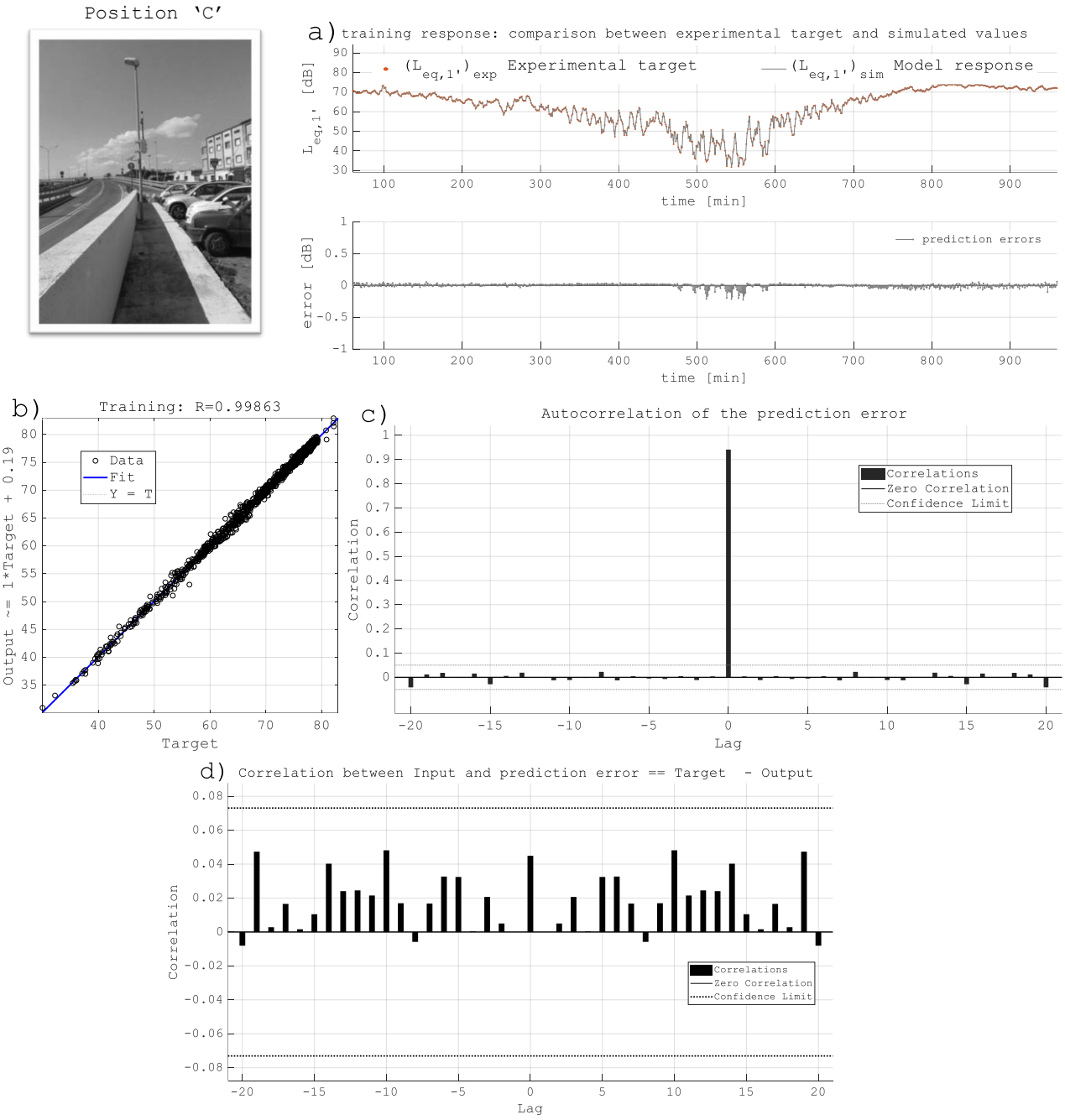

Fig. 10 Training performances for experimental data measured at point C. In a) comparison and prediction error of simulated and measured $L_{A,eq,1'}$; b) regression between traffic input and acoustic output sequences; c) autocorrelation function of the prediction error sequence. d) cross-correlation function between prediction error and traffic input sequence.

5.2 Testing process

In this section the relevant results of the testing processes of the NARX model are reported. The model has been tested adopting the closed loop architecture (illustrated in Fig. 4a) that performs multi-step ahead predictions where the values predicted in the preceding steps (output feedback) are used as input for predicting multi time steps ahead.

The ability of the NARX model to generalize what has been learned from the training subset has been verified on a large test set size, composed (at the least) of a sequence of 7690 records, corresponding to 89% of the experimental observations. The training set is much smaller and contains the remaining 11%.

These values should not be overlooked since the model's generalization ability robustness relies to some extent, on the adopted percentages composition of the training and testing sets.

In pattern recognition or time series prediction, the training set is usually larger than the test set. The recommended percentages, reported in standard applications, being close to 80% and 20% respectively. Training sets composed of less than 80% of the experimental data may be inadequate, they likely contain too little information to achieve good generalization of learning across all the experimental observations.

Consequently, successful generalization performance (namely attaining small prediction errors) becomes an increasingly formidable task as the size of the training set size diminishes and thus the test set increases. However, on the other hand, it is also true, that the statistical consistency of the prediction capability would be strengthened.

Vice versa, increasing the training set to more than 80% facilitates achieving small prediction errors, may nevertheless undermine the statistical consistency of the generalization power. Therefore, a suitable division should reflect a compromise between the requirements (frequently conflicting) of reducing the prediction errors and increasing the size of the test set for enhancing the robustness of the generalization capability.

The test results are divided into two separate time periods, the three off-season days in March 2019 and the three days during the peak tourism season in August 2019.

Figures 11, 12 and 13, provide a representative picture of the ability of the neural model to generalize the traffic - noise relationship across the entire measurement periods and for traffic inputs not used to train the network.

The numerical results, represented by the solid grey curves in Figures 11b-13b, are obtained using the model for generating multistep-ahead predictions of the test set samples. In particular, any point at a given instant of the grey curves is a simulated predicted value and is generated by using, as input regressors, the noise level predictions generated at previous instants in combination with the experimental values of the traffic data.

Therefore, the experimental values of the noise level are not used by the model for predicting the grey curves, but rather are depicted, with the dotted blue curves in the graph, only for comparison with the simulated values.

The prediction error between the response of the model $L_{eq,1',sim}$ and the experimental target $L_{eq,1',exp}$ for vehicle traffic input data not included in the training set is shown in the sub-plots of figs. 11, 12 and 13. Figs. 11 - 13 show how the model is well adapted over the complete measuring periods. Moreover, since satisfactory generalization performances of the learning process have been attained on a large size of the test subset size, in spite of the relatively small size of the training set, the achieved generalization capability could be considered reliable.

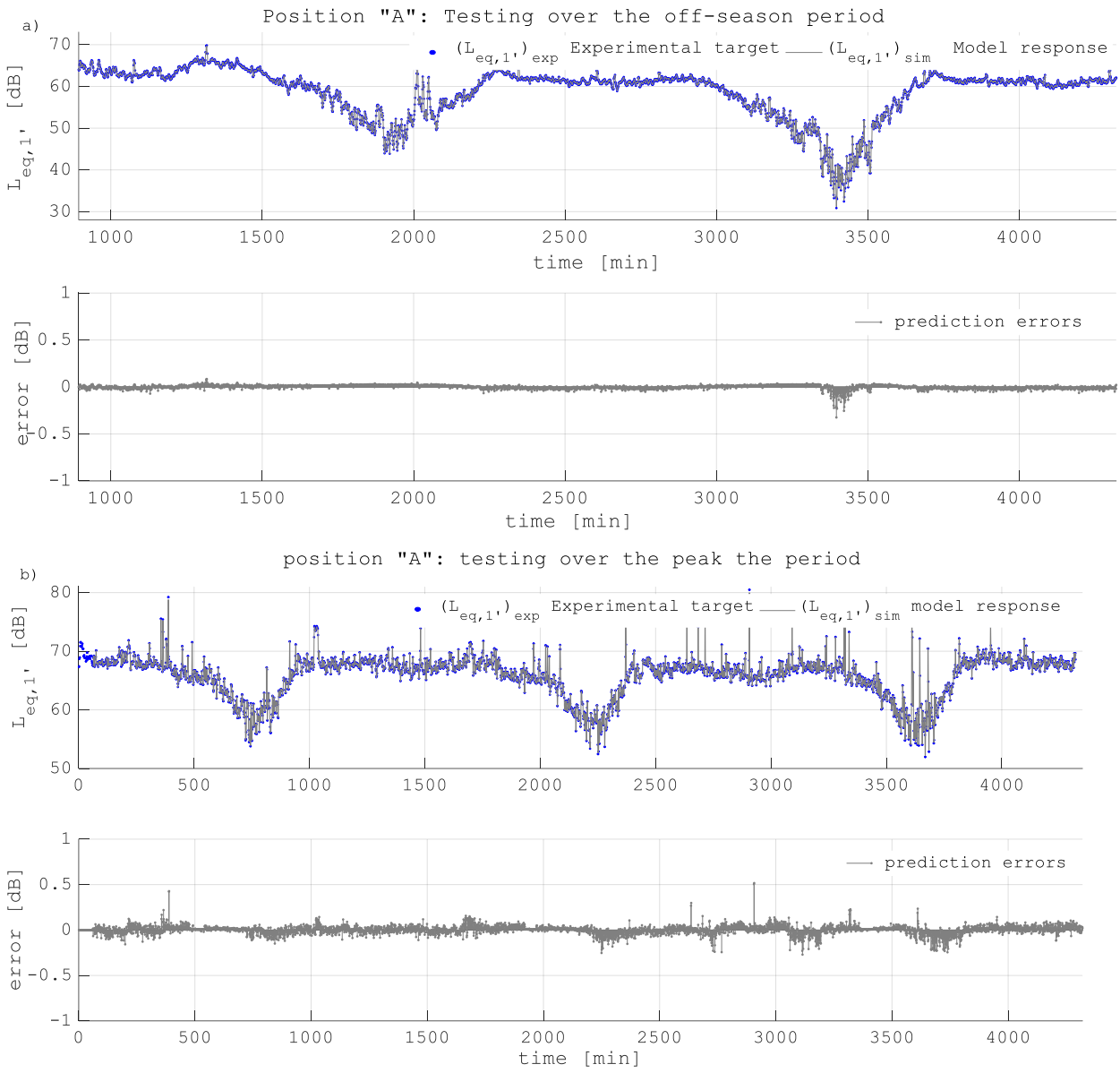

Fig. 11. Simulated and experimental evolution of $L_{eq,1'}(\tau)$, at measurement point **A**. In a) during off- season (March) and in b) during peak season (August) traffic flow rates. The comparison is performed across the measurement period of the test datasets sequence.

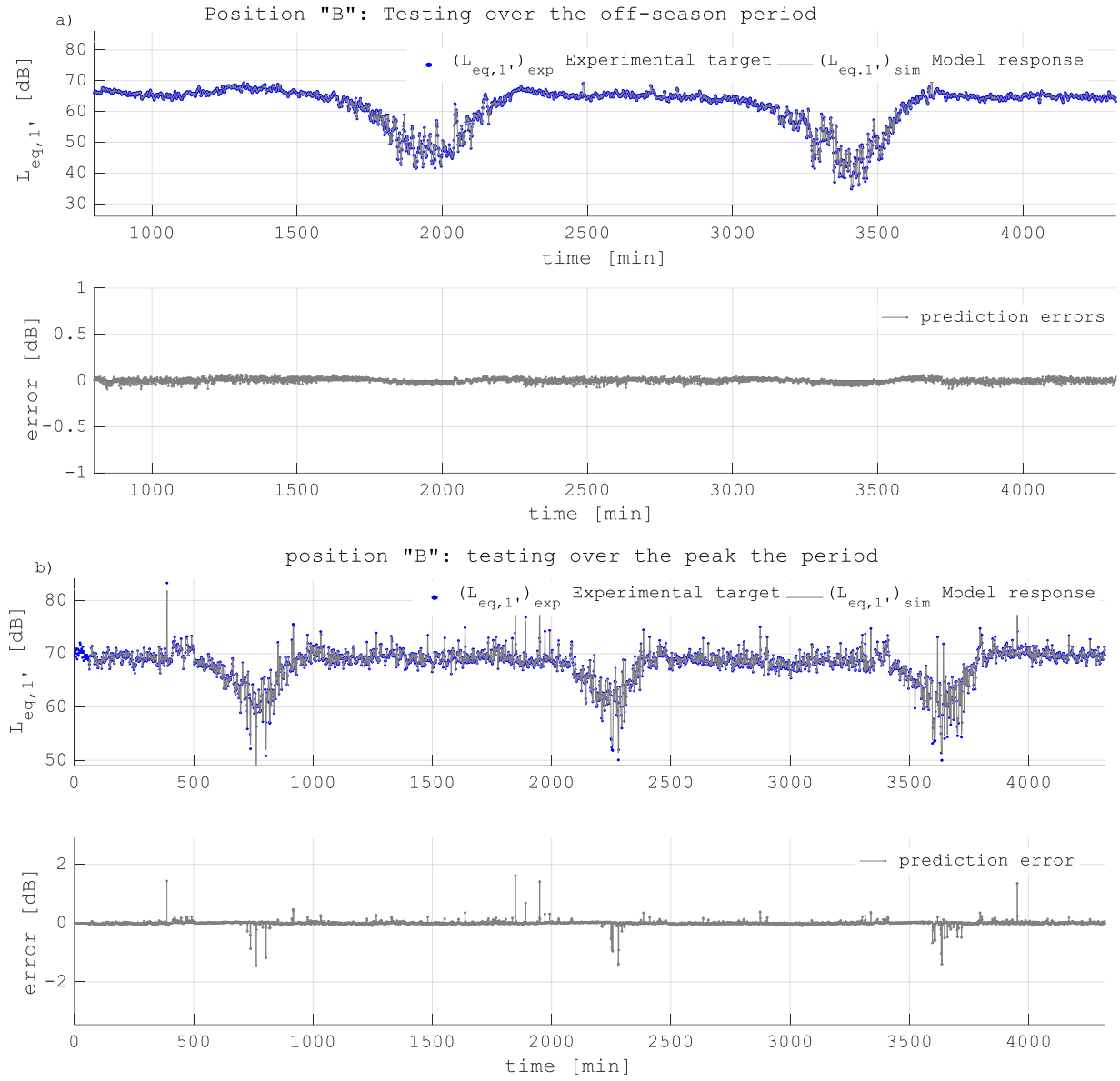

Fig. 12. Simulated and experimental evolution of $L_{eq,1'}(\tau)$, at measurement point **B**. In a) during off- season (March) and in b) during peak season (August) traffic flow rates. The comparison is performed across the measurement period of the test datasets sequence.

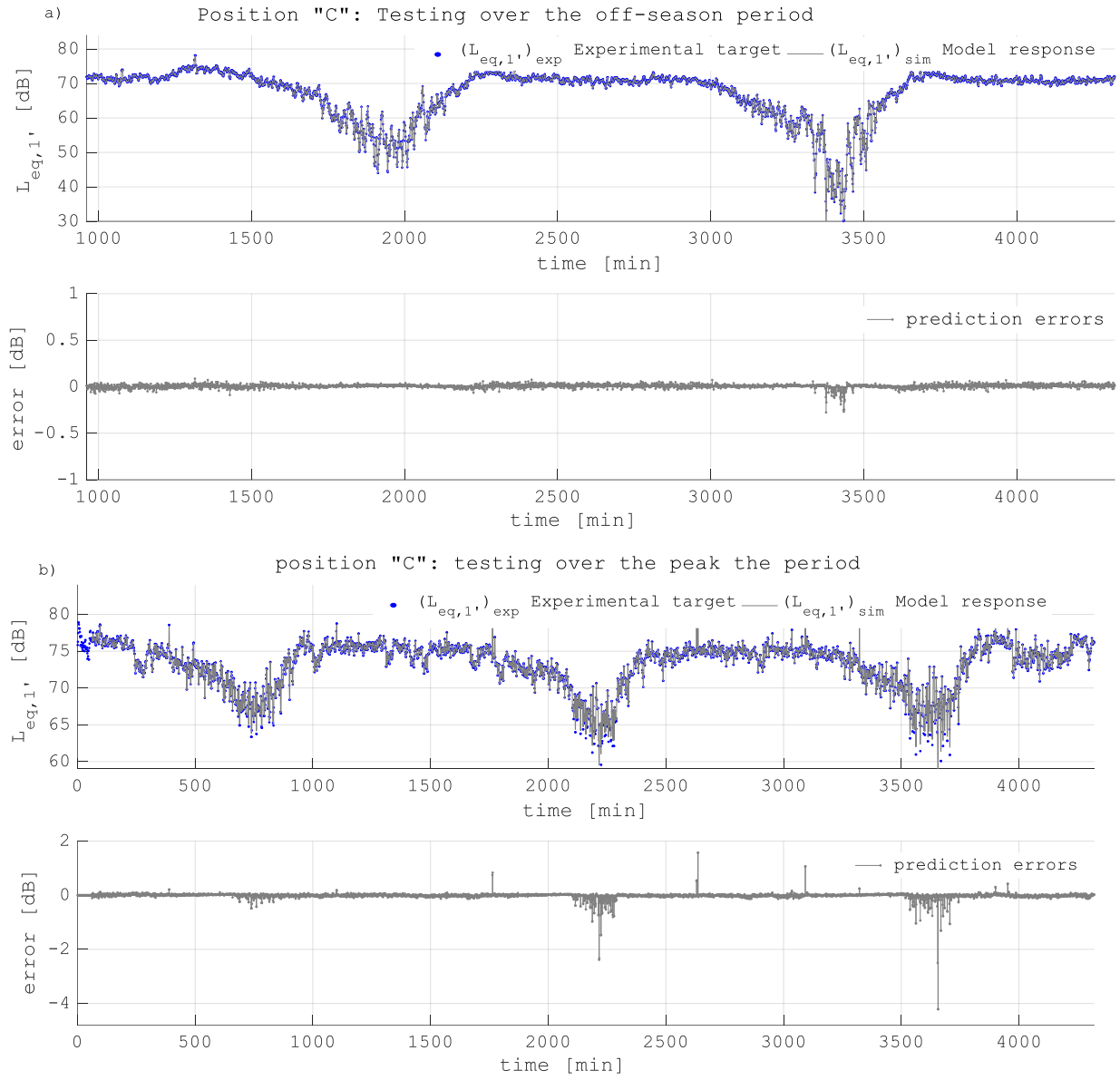

Fig. 13. Simulated and experimental evolution of $L_{eq,1'}(\tau)$, at measurement point **C**. In a) during off- season (March) and in b) during peak season (August) traffic flow rates. The comparison is performed across the measurement period of the test datasets sequence.

Table 1 provides insight into the model's performances. Different measures of the noise level prediction error at the measurement points A, B and C are shown for both measurement periods. The most widely used key performance indicators (KPI) have been considered, namely the mean absolute error (MAE), the mean absolute percentage error (MAPE) and the root mean squared error (RMSE).

Table 1.
Different measures of the prediction error of the noise level at the measurement points A and C: mean absolute error (MAE), mean absolute percentage error (MAPE) and root mean squared error (RMSE)

Position	Season	MAE	MAPE	RMSE
A	off-season	1,727E-02	3,151E-04	2,772E-02
	peak period	3,250E-02	5,123E-04	4,559E-02
B	off-season	1,971E-02	3,308E-04	2,483E-02
	peak period	2,883E-02	4,518E-04	6,512E-02
C	off-season	1,624E-02	2,484E-04	2,322E-02
	peak period	5,962E-02	8,671E-04	1,092E-01

Table 1 reflects the overall behavior of the prediction error curves represented in Figs 11 – 13. Indeed, the RMSE indicator displays greater values than the other KPI because it emphasizes the most significant errors, while the others give the same importance to each error value.

Anticipating the results discussed in the next section, it is clear from table 1 that the model exhibits small mean prediction errors and during the off-season period of the traffic flow rate it performs consistently better for all indicators of the prediction error.

6. Test results and discussion

As can be observed from the graphs depicted in Figs. 8a - 10a, and 11 – 13, the model performs well in predicting the temporal evolution of the sound pressure levels generated by road traffic at the three points A, B and C. Indeed, the temporal evolution of $L_{eq,1'}(\tau)$ predicted by the neural model fits the experimental data, measured across the entire timeline of the measurement periods, fairly well.

The training and the generalization processes were performed on a training and a test set containing from 800 to 950 records and from 7840 to 7690 records respectively, corresponding to 9% - 11% (for the training set) and 91% – 89% (for the test set) of the experimental observations. Clearly, the test set records were not included in the training process but were subsequently considered for verifying the ability to generalize training on other configurations.

Figures 11, 12 and 13 demonstrate the good prediction ability, during validation of the testing stage, across all the reference time intervals considered (day, evening, and nighttime) for both the off-season (Figs 11a, 12a and 13a) and peak season traffic conditions (Figs 11b, 12b and 13b) and at all the "measurement points A", B and C. In particular, the prediction error profile entirely lies within the range ±0.5dB throughout the off-season traffic period at all the measurement points but only at A during the peak season traffic conditions.

Though during peak season traffic the prediction error at "measurement points B and C falls largely within the range ±0.5dB, in several instances the error increases, especially at nighttime. The discrepancy observed between experimental and simulated values may be attributed to the additional components of non-traffic related noise events, or anomalous noise events (ANEs). Indeed, the substantial increase in evening and nighttime noise levels can likely be explained by the influx of tourists in the port city, while intermittent average reductions in traffic flows are observed. The trends of the autocorrelation function of the prediction error sequence and the cross-correlation function between the input traffic data and the prediction error sequences shown in Figures 8, 9 and 10 (boxes c and d), warrant consideration. The autocorrelation function reveals a negligible (close to zero) correlation for all non-zero lags at the three measurement points, whereas the cross-correlation function takes negligible values for all lags. This behavior suggests that the identified prediction model is an appropriate candidate for explaining the functional dependence of the traffic-noise-relationship. As concerns the measurement points the results can be summarized as follows:

Off-season measurement period at point A, Figs. 8-11, boxes a):

training set performance: the prediction error between the experimental and computed values is always lower than 0.5 dB

test set performance: the prediction error between the experimental and computed values is always lower than 0.5 dB.

Peak traffic measurement period at point A, Fig. 11, box b)

test set performance: the prediction error between the experimental and computed values is lower than 0.5 dB almost everywhere except for few records where the error is slightly higher than 0.5 dB.

Off-season measurement period at point B, Figs. 9-12, boxes a)

Training set performance: the prediction error between the experimental and computed values is always lower than 0.2 dB.

Test set performance: the prediction error between the experimental and computed values is always lower than 0.15 dB.

Peak traffic measurement period at point B, Fig. 12, box b)

Test set performance: the prediction error between the experimental and computed values is lower than 0.5 dB almost everywhere, except during certain time periods when the error occasionally slightly exceeds 1.5 dB.

Off-season measurement period at point C, Figs. 10-13, boxes a)

Training test performance: the prediction error between the experimental and computed values is always lower than 0.5 dB.

Test set performance: the prediction error between the experimental and computed values is always lower than 0.5 dB.

Peak traffic measurement period at point C, Fig. 13, box b)

Test set performance: the prediction error between the experimental and computed values is lower than 0.5 dB almost everywhere, except for few records where the error slightly exceeds 1, 2 and 4 dB.

Though the model results are satisfactory for all three measurement points and for the two periods considered, a slight deterioration in the prediction error can be observed for all three points during the peak season. This trend can be reasonably explained by the increase in the number of people around in the evening and at nighttime in August compared to March. Indeed, during the height of the tourist season pedestrians flock to the shops, restaurants etc. along and near the waterfront that stay open until late. Thus, the noise sources associated with the flow of pedestrians to/in outdoor meeting places become superimposed on traffic noise. The above considerations are confirmed by the poorer performance in the saddle points between evening and nighttime when the city's waterfront attracts crowds of tourists. However, the deterioration in performance is only marginal if compared to the overall generalization ability of the model and the amount of perturbations generated by humans that cannot be ascribed to traffic. This aspect confirms the ability of the model to single out, to a certain extent, vehicle traffic even in the presence of additional environmental background noise.

The feedback input of the acoustic noise regressors and a training sequence that covers a portion of the nighttime period could have played a key role in accounting for the presence of the additional stationary noise across the measurement period. The model was able to predict $L_{eq,1'}$ values close to the noise levels recorded in the three measurement points under different environmental, traffic and background noise conditions. This behavior was observed both in the off-season and peak tourist season and for signals recorded in quasi-stationary and highly variable conditions. Further, traffic behaves differently depending on the measurement point. At point C traffic moves smoothly with vehicles traveling at practically constant speed, while at the roundabout at point A vehicle flow is intermittent on the approach road and in congested traffic. Lastly, at the signalized intersection at point B traffic is discontinuous and other sources of noise are caused by the restaurants, bars and shops in the vicinity.

7. Conclusions

Areas in the vicinity of port cities are often exposed to traffic noise fluctuations, associated with access to and from the port of large volumes of vehicular traffic, especially during the tourist season. This has an adverse impact on the livability of the neighbouring urban areas.

The acoustical context that is under consideration in the present study, is strongly influenced by the tourist traffic flows and port activities whose large variability cannot be easily delineated by a priori characterization.

The present study describes an adaptive identification neural network model developed for dynamically predicting the acoustic noise from vehicular traffic in a port city waterfront. The model is based on a NARX architecture and has been trained and successfully tested using experimental acoustic noise levels and traffic composition data measured during off-season and peak tourist season. Traffic in fifteen road lanes and acoustic pressure levels at three measurement points, representative of the acoustic field in the urban waterfront area, are considered for identifying the prediction model.

Clearly, one important point needs to be clarified. The model we developed is not based on a particular modelling technique of specific structural aspects of waterfronts in port cities and cannot therefore be

construed as an approach used exclusively for solving road noise issues in those contexts. Actually, the experimental noise levels and traffic data used in the training phase means the model is tailored to the specific context of the case study. However, this does not mean that the modeling framework can be implemented solely in waterfront contexts. Rather, the architecture of the NARX model proved a valid choice for our context where dynamics, accuracy, small time refinement and computation efficiency are decisive, and did not require incorporating specific aspects of waterfronts in port cities into the model. It is precisely for this reason that the methodological framework can be easily extended to contexts other than waterfronts, where in any case these features prove to be essential for solving road noise issues.

The following results, worthy of note, can be drawn from this exploratory investigation.

- The model developed here provides simulations with a short time refinement of one minute while exhibiting smaller prediction errors than those obtained in earlier studies. Indeed, the discrepancy range between the predicted and the experimental temporal profile of the noise level lies almost everywhere within the range ±0.5 dB, almost everywhere, except for few instances at nighttime in the peak traffic period at measurement points B and C, where the prediction error is occasionally slightly larger. However, the identified model exhibits a good quantitative agreement with the experimental values since the predicted time series $L_{eq,1',sim}$ generated by the NARX model, broadly matches the experimental profile $L_{eq,1',exp}$ of the measured noise levels, over both the characterizing periods and for the training as well as the test sets, during daytime, evening and nighttime, seamlessly.
- The good prediction power of the developed model (in generalizing what has been learned from the training subset) has been demonstrated on a large test set size, despite the relatively small size of the training set. Specifically in the present investigation, a training sequence of $L_{eq,1'}(\tau)$ measured during transient conditions, composed of about 900 minutes (~11%) and strictly synchronized with detailed traffic data, proved to be sufficient for predicting, with a good quantitative agreement, the evolution of $L_{eq,1'}$ measured in three different positions over a time span ten times larger, (~7700 minutes corresponding to ~89% of the whole experimental data set, spanning from off-season to peak traffic period). This result suggests that the generalization ability of the model is reliable and rests on a training set representative of the experimental observations. In other words, the experimental observations incorporated in the training set, being characterized by an ample transitoriness, are fairly representative of the sample space generable by the traffic-noise event at the selected measurement points in the waterfront area.

This feature deserves to be not under evaluated as achieving small prediction errors on a statistically consistent test set size is an attractive overarching objective that dominates the development procedure of a prediction model. In many earlier studies the prediction ability has been validated on a small portion, at the most 30%, of the entire data set. In many others, the overall consistency of the generalization ability of the proposed model cannot be assessed since no information about the composition of the training, validation and test sets is provided.

- The appropriateness of the identification model is also borne out by the profile of the autocorrelation and cross-correlation functions of the prediction error and the traffic data sequences. The behavior of these

functions supports the hypothesis that the model identified is able to explain the functional dependence, such that the same data generation mechanism exhibited by the actual traffic noise event can be re-proposed.

The model developed in this exploratory investigation, is a preliminary step for defining short term strategies, responsive in a short time scale, aiming to reduce traffic noise emissions in port cities' waterfronts. The study is focused on identifying a cause-effect model that is able to describe the action exerted by the traffic variables (causal exogenous input variables) on the output effect variables (noise level), with a sub hourly temporal refinement.

The model can be employed for achieving two different and possibly complementary tasks: a) optimization / simulation and b) monitoring purposes.

a) In the first case the model could be used as a simulation tool for designing a series of optimal traffic management strategies and for predicting their impact on noise level reduction.

In effect, if different patterns of the traffic flow explanatory variables are used as model input, the corresponding output can be analyzed for capturing how different simulated traffic scenarios impact on the corresponding simulated noise level.

Therefore, by iterating and evaluating alternative configurations of simulated input traffic flow, until the desired noise abatement is achieved, acoustic engineers and transport planners can drive the model with optimized input configurations to satisfy specific optimization criteria. The formulation of optimized management strategies that recommend driving behavior and routes, for optimizing traffic flow and prioritization and consequently alleviating noise in specific susceptible areas will be addressed in a future study.

b) Once a set of optimal traffic flow configurations has been defined the model can be used in the field for monitoring purposes. Simply using traffic flow measurements, the model can be used for monitoring road traffic noise as traffic flows change over time. The temporal profile of the predicted noise level together with the experimental traffic data provide the information source from which specific features can be extracted for driving the decision-making process to evaluate if and how the traffic should be reorganized on the basis of the previously designed optimal configurations. In this phase sound pressure level measurements can be omitted so the measurement campaign can be minimized and used simply for tuning the model. Note that in monetary terms the savings are appreciable, as the cost per unit of noise level measurements is higher than for traffic counts and what is more many cities are already equipped with traffic volume counters for traffic flow planning and management.

The results presented here concern the acoustic environment and traffic scenarios in a specific city and they cannot be generalized to other localities. An interesting development would be to extend the methodology to other waterfront cities.

Acknowledgements

This work has received partial financial support from Interreg Italy France- Maritime program, which is gratefully acknowledged. The funder had no role in study design, data collection and analysis, decision to publish, or preparation of the manuscript.

References

[1] Reported data on noise exposure covered by Directive 2002/49/EC: Exposure of Europe's population to environmental noise Number of people exposed to average day-evening-night noise levels (Lden) ≥ 55 dB and to night-time noise (Lnight) ≥ 50 dB in in Europe.

[2] M. Hornikx, Advances in environmental acoustics, Building and Environment, Volume 154 (2019) A1-A2, ISSN 0360-1323, https://doi.org/10.1016/j.buildenv.2019.03.055.

[3] X. Li, S.K. Tang, S.Y.C. Yim, R.Y.C. Lee, T. Hung, Noise reduction of plenum windows on the façade of a high-rise residential building next to heavy road traffic, Building and Environment, 186 (2020) 1-12, ISSN 0360-1323, https://doi.org/10.1016/j.buildenv.2020.107353.

[4] C. Anon, Handbook of acoustic noise control WADC technical report, 52-204. Wright Air Development Center, 1952.

[5] H. Bendtsen, The Nordic prediction method for road traffic noise, Science of The Total Environment, 235 (1999) 331-338, Issues 1–3, ISSN 0048-9697, https://doi.org/10.1016/S0048-9697(99)00216-8.

[6] D. Borelli, S. Repetto, C. Schenone, Noise mapping of the flyover highway in Genoa: Comparison of different methods 1(2014) 59-73, Noise Mapping, 1 (1), DOI: 10.2478/noise-2014-0007.

[7] J. Quartieri, N. E. Astorakis, G. Iannone, C. Guarnaccia,S. D'Ambrosio, A. Trois, TLL Lenza, Review of traffic noise predictive models Recent Advances, Applied And Theoretical Mechanics 5 (4) (2011) 379-386.

[8] S. Abo-Qudais, A. Alhiary, Statistical models for traffic noise at signalized intersections, Building and Environment, 42(2007) 2939-2948, ISSN 0360-1323, https://doi.org/10.1016/j.buildenv.2005.05.040.

[9] N. Garg, S. Maji, A critical review of principal traffic noise models: Strategies and implications, Environmental Impact Assessment Review, 46 (2014) 68-81, ISSN 0195-9255, https://doi.org/10.1016/j.eiar.2014.02.001.

[10] J. Quartieri, N. E. astorakis, G. Iannone, C. Guarnaccia,S. D'Ambrosio, A. Trois, TLL Lenza, Review of traffic noise predictive models Recent Advances In Applied And Theoretical Mechanics 2009.

[11] C. Guarnaccia, T.L.L. Lenza, N.E. Mastorakis, J. Quartieri A comparison between traffic noise experimental data and predictive models results. Int. J. Mech., 5 (4) (2011) 379-386.

[12] C. Steele, A critical review of some traffic noise prediction models, Applied Acoustics, 62 (3) (2001) 271-287, ISSN 0003-682X, https://doi.org/10.1016/S0003-682X(00)00030-X.

[13] A. Can, L. Leclercq, J. Lelong, J. Defrance, Accounting for traffic dynamics improves noise assessment: Experimental evidence, Applied Acoustics, 70 (6) (2009) 821-829, ISSN 0003-682X, https://doi.org/10.1016/j.apacoust.2008.09.020.

[14] L. Leclercq, J. Lelong, Dynamic evaluation of urban traffic noise, Proceedings of the 17th international congress on acoustics, Rome, 2001.

[15] B. De Coensel, T. Demuer, I. Yperman, D. Botteldoren, The influence of traffic flow dynamics on urban soundscape.

[16] A. Can, L. Leclercq, J. Lelong, J. Defrance, Capturing urban traffic noise dynamics through relevant descriptors, Applied Acoustics, 69 (12) (2008) 1270-1280, ISSN 0003-682X, https://doi.org/10.1016/j.apacoust.2007.09.006.

[17] L. Estévez-Mauriz, J. Forssén, Dynamic traffic noise assessment tool: A comparative study between a roundabout and a signalized intersection, Applied Acoustics 130 (2018) 71-86, ISSN 0003-682X, https://doi.org/10.1016/j.apacoust.2017.09.003.
[18] A. Can, L. Leclercq, J. Lelong, Dynamic estimation of urban traffic noise: Influence of traffic and noise source representations, Applied Acoustics 69 (10) (2008) 858-867, ISSN 0003-682X, https://doi.org/10.1016/j.apacoust.2007.05.014.
[19] A. Can, L. Leclercq, J. Lelong, J. Defrance, Accounting for traffic dynamics improves noise assessment: Experimental evidence, Applied Acoustics 70 (6) (2009) 821-829, ISSN 0003-682X, https://doi.org/10.1016/j.apacoust.2008.09.020.
[20] A. Can, L. Leclercq, J. Lelong, D. Botteldooren, Traffic noise spectrum analysis: Dynamic modeling vs. experimental observations, Applied Acoustics 71 (8) (2010) 764-770, ISSN 0003-682X, https://doi.org/10.1016/j.apacoust.2010.04.002.
[21] L. Estévez-Mauriz, J. Forssén, Dynamic traffic noise assessment tool: A comparative study between a roundabout and a signalised intersection, Applied Acoustics, 130 (2018), 71-86, DOI: 10.1016/j.apacoust.2017.09.003.
[22] R. Benocci, A. Molteni, M. Cambiaghi, F. Angelini, H. Eduardo Roman, G. Zambon, Reliability of Dynamap traffic noise prediction, Applied Acoustics 156 (2019) (142-150), ISSN 0003-682X, https://doi.org/10.1016/j.apacoust.2019.07.004.
[23] Q. Hou, M. Cai, H. Wang, Dynamic modeling of traffic noise in both indoor and outdoor environments by using a ray tracing method, Building and Environment 121 (2017) 225-237, ISSN 0360-1323, https://doi.org/10.1016/j.buildenv.2017.05.031.
[24] G. Rey Gozalo, P. Aumond, A. Can, Variability in sound power levels: Implications for static and dynamic traffic models, Transportation Research Part D: Transport and Environment 84 (2020), ISSN 1361-9209, https://doi.org/10.1016/j.trd.2020.102339.
[25] M. Hornikx, Ten questions concerning computational urban acoustics, Building and Environment 106 (2016) 409-421, ISSN 0360-1323, https://doi.org/10.1016/j.buildenv.2016.06.028.
[26] M. Hornikx, J. Forssén, Modelling of sound propagation to three-dimensional urban courtyards using the extended fourier PSTD method, Applied Acoustics 72 (9) (2011) 665-676, ISSN 0003-682X, https://doi.org/10.1016/j.apacoust.2011.03.005.
[27] H. Wang, H. Gao, M. Cai, Simulation of traffic noise both indoors and outdoors based on an integrated geometric acoustics method, Building and Environment 160 (2019) 106-117, ISSN 0360-1323, https://doi.org/10.1016/j.buildenv.2019.106201.
[28] L. Bravo-Moncayo, J. Lucio-Naranjo, M. Chávez, I. Pavón-García, C. Garzón, A machine learning approach for traffic-noise annoyance assessment, Applied Acoustics 156 (2019) 262-270, ISSN 0003-682X, https://doi.org/10.1016/j.apacoust.2019.07.010.
[29] N. Genaro, A. Torija A. Ramos-Ridao I. Requena D. P. Ruiz M. Zamorano A neural network based model for urban noise prediction The Journal of the Acoustical Society of America 128 (1738) (2010), https://doi.org/10.1121/1.3473692.
[30] V. Nourani, H. Gökçekuş, I. Khalil Umar, Artificial intelligence-based ensemble model for prediction of vehicular traffic noise, Environmental Research 180 (2020), 108-122, ISSN 0013-9351, https://doi.org/10.1016/j.envres.2019.108852.
[31] Ali Khalil M, Hamad K, Shanableh A. Developing Machine Learning Models to Predict Roadway Traffic Noise: An Opportunity to Escape Conventional Techniques. Transportation Research Record. 2019;2673(4):158-172. doi:10.1177/0361198119838514
[32] A. Sharma, R. Vijay, G. L. Bodhe, et al., An adaptive neuro-fuzzy interface system model for traffic classification and noise prediction, Soft Comput 22 (2018) 1891–1902, https://doi.org/10.1007/s00500-016-2444-z.

[33] J. Tomić, N. Bogojević, M. Pljakić, D. Šumarac-Pavlović, Assessment of traffic noise levels in urban areas using different soft computing techniques, The Journal of the Acoustical Society of America 140 (2016), https://doi.org/10.1121/1.4964786.
[34] N. Garg, P. Dhiman, S. K. Mangal, Comparison of ANN and analytical models in traffic noise modeling and predictions, International Journal of Artificial Intelligence and Neural Networks 4 (3) (2014) 2250-3749.
[35] G. Cammarata, S. Cavalieri, A. Fichera, A neural network architecture for noise prediction, Neural Networks, 8 (6) (1995) 963-973, ISSN 0893-6080, https://doi.org/10.1016/0893-6080(95)00016-S.
[36] Cammarata G., Cavalieri S., Fichera A., Marletta L. (1993) Noise prediction in urban traffic by a neural approach. New Trends in Neural Computation - IWANN 1993 Lecture Notes in Computer Science 686, Springer, Berlin, Heidelberg, https://doi.org/10.1007/3-540-56798-4_210.
[37] V. Nedic, D. Despotovic, S. Cvetanovic, M. Despotovic, S. Babic, Comparison of classical statistical methods and artificial neural network in traffic noise prediction, Environmental Impact Assessment Review 49 (2014) 24-30, ISSN 0195-9255, https://doi.org/10.1016/j.eiar.2014.06.004.
[38] A.J. Torija, D.P. Ruiz, A.F. Ramos-Ridao, Use of back-propagation neural networks to predict both level and temporal-spectral composition of sound pressure in urban sound environments, Building and Environment 52 (2012) 45-56, ISSN 0360-1323, https://doi.org/10.1016/j.buildenv.2011.12.024.
[39] K. Hamad, M.A. Khalil, A. Shanableh, Modeling roadway traffic noise in a hot climate using artificial neural networks, Transportation Research Part D: Transport and Environment 53 (2017) 161-177, ISSN 1361-9209, https://doi.org/10.1016/j.trd.2017.04.014.
[40] V. Nourani, H. Gökçekuş, I.K. Umar, H.Najafi, An emotional artificial neural network for prediction of vehicular traffic noise, Science of The Total Environment 707 (2020) 136-154, ISSN 0048-9697, https://doi.org/10.1016/j.scitotenv.2019.136134.
[41] P. Kumar, S.P. Nigam, N. Kumar, Vehicular traffic noise modeling using artificial neural network approach, Transportation Research Part C: Emerging Technologies 40 (2014) 111-122, ISSN 0968-090X, https://doi.org/10.1016/j.trc.2014.01.006.
[42] L. Chen, B. Tang, T. Liu, H. Xiang, Q. Sheng, H. Gong, Modeling traffic noise in a mountainous city using artificial neural networks and gradient correction, Transportation Research Part D: Transport and Environment 78 (2020) 182-196, ISSN 1361-9209, https://doi.org/10.1016/j.trd.2019.11.025.
[43] S. Givargis, H. Karimi, A basic neural traffic noise prediction model for Tehran's roads, Journal of Environmental Management 91 (12) (2010) 2529-2534, ISSN 0301-4797, https://doi.org/10.1016/j.jenvman.2010.07.011.
[44] D. Singh, S.P. Nigam, V.P. Agrawal, M. Kumar, Vehicular traffic noise prediction using soft computing approach, Journal of Environmental Management 183 (1) (2016) 59-66, ISSN 0301-4797, https://doi.org/10.1016/j.jenvman.2016.08.053.
[45] C. Schenone, I. Pittaluga, S. Repetto, D. Borelli, Noise pollution management in ports: A brief review and the EU MESP project experience, 21st International Congress on Sound and Vibration 2014.
[46] L.R. Medsker and L.S. Jain, Recurrent Neural Networks: Design and Applications, The CRS Press International Series on Computational Intelligence 2000.
[47] S.A. Billings, Nonlinear System Identification: NARMAX Methods in the Time, Frequency, and Spatio-Temporal Domains, Wiley, ISBN: 978-1-118-53555-4 July 2013.
[48] D. Marquardt, An Algorithm for Least-Squares Estimation of Nonlinear Parameters, SIAM Journal on Applied Mathematics 11 (2) (1963) 431–441.
[49] M.T. Hagan, and M. Menhaj, Training feed-forward networks with the Marquardt algorithm, IEEE Transactions on Neural Networks 5 (6) (1999) 989–993.